



**UNIVERSITY of the  
WESTERN CAPE**

**Screening of Selected Libyan Medicinal Plants for the  
Synthesis of Metal Nanoparticles and their activity against  
*Streptococcus mutans***

**Salah Ramadan Alshibani**

Student Number: 3581006

*A thesis submitted in fulfilment of the requirements for the degree*

**Magister Scientiae (MSc)**

**Department of Medical Biosciences**

**Faculty of Natural Sciences**

**University of the Western Cape**

**Supervisor**

**Prof Ahmed Mohammed**

**Co supervisor**

**Prof Donavon Hiss**

**November 2019**

## DECLARATION

I, Salah Ramadan Alshibani, declare that “**Screening of Selected Libyan Medicinal Plants for the Synthesis of Metal Nanoparticles and their activity against *Streptococcus mutans***” is ‘original work and that all the sources that I have used or cited have been indicated and acknowledged by means of complete references, and that this document has not been submitted for degree purposes at any other academic institution

**Salah Ramadan Alshibani**

A handwritten signature in dark ink, enclosed within a light blue rectangular border. The signature is stylized and appears to read 'Salah'.

Student Number: 3581006

**Date Signed 21/11/2019**

## DEDICATION

*This study is dedicated to my Wife, Hend, My children, Raghad, Abdel Moneim, Mohammed, and small Yara*

## ACKNOWLEDGEMENTS

*First, thank God Almighty who helped me and ridiculed me to reach this point*

*In particular, I would like to thank my supervisor, Pro Ahmed Mohamed, for all care, patience, support, and guidance. It was your time invested in me and the words were really encouraging in vain. I would also like to thank my co-supervisor, Pro Donavon Hiss, for his support and willingness to help in difficult times*

*I would like to thank my supervisors for giving me the opportunity to follow this exciting study and for all your help and guidance throughout the process, although I was not a very easy student, I am forever grateful*

*I would like to thank Professor Mervin Meyer for helping me with biological study and allowing me to conduct all my biological experiments in his laboratory.*

*A special Thanks to Dr. Ismail for her assistance and contribution during the writing of the thesis*

*To Dr, Mustafa Edrah, Abdul Rahman Al-Bagouri. I am very grateful for all your help, patience, and continued support. I do not forget Dr, Nicole Seaboy, who is Sister Nicole to us*

*My colleagues in the department for their advice, assistance and motivation*

*Last but not least, to my wife and children, to all their love, support, prayers, motivation, words of encouragement. Thank you for your help and other family members for their support and friends who have stood with me in difficult times. I am really grateful for all your support*

## ABSTRACT

Nanotechnology has emerged as an elementary division of modern science and stemmed directly from green chemistry twelve basic concepts, it receives global attention due to its unique character and ample applications. It also has great potential to mitigate the challenges they face in various fields, especially medical sector. Nanodrugs are increasingly considered as a potential candidate to carry therapeutic agents safely into a targeted compartment in an organ, particular tissue or cell.

In this study, twenty (20) Libyan plants were selected and evaluated for their potential to synthesis gold and silver nanoparticles. The screening of the different plant extracts was performed using 96 well plate method at 25 °C and 70 °C. The NPs formation was confirmed and characterized using UV- Vis, DLS, HR-TEM and EDX. A well-defined NPs were obtained at high temperature (70 °C).

The Au NPs had an average diameter of 92 nm at 25 °C and 66 nm at 70 °C. The zeta potential values were observed to be negative (-14 to -24) and indicate the stability of the Au NPs. The HR-TEM showed polydispersity, which decreased at higher temperature (70 °C). The stability of Au NPs in nutrient broth prior was conducted as well. All the Au NPs under study showed stability, only minimal changes in the UV-Vis spectra can be observed. Two plant extract *viz Pistacia atlantica, Junipers phoenicea* showed consistent results and forming stable and smaller NPs compared to others, both of the plant extracts and the corresponding NPs were tested against *Streptococcus mutans* and showed MIC value ~ 49 µg/mL.

In case of silver NPs, two plant extracts *viz J. phoenicea, Rosmarinus officinalis*, showed superior results than the others; both plants produced stable and small Ag NPs. The antibacterial activity against *S. mutans* demonstrated MIC valus ~ 50 µg/mL.

The synthesised NPs showed a promising bioactivity for developments of new antibacterial agents against *S. mutans* strains. Dose-dependent activity was observed for the tested NPs.

The obtained results gave insight into the importance of the natural products as efficient method for preparation of new bioactive and safe alternative treatment for different human pathologies including bacterial infection.

**Keywords:**

Nano-biotechnology, Libyan medical flora, Plant extract, Antibacterial activity, Gold nanoparticles, Silver nanoparticles, Dental caries, *Streptococcus mutans*

## LIST OF ABBREVIATIONS

<b>Ag NP<sub>s</sub></b>	Silver nanoparticles
<b>Au NPs</b>	Gold nanoparticles
<b>dH<sub>2</sub>O</b>	Distal water
<b>DLS</b>	Dynamic Light Scattering
<b>EDX</b>	Energy dispersive X- ray spectroscopy
<b>GNPs</b>	Green Nanoparticles (gold and/or silver)
<b>NPs</b>	Nanoparticles
<b>OC</b>	Optimum concentration
<b>TEM</b>	Transmission Electron Microscopy
<b>UV-Vis</b>	Ultra Violet-Visible Spectroscopy
<b>ZP</b>	Zeta Potential
<b>MIC</b>	Minimum inhibitory concentration

# Table of Contents

	Page
Title page	i
Declaration	ii
Dedication	iii
Acknowledgements	iv
Abstract	vi
List of abbreviations	viii
Contents	ix
List of figures	
List of tables	
Chapter 1/ Introduction	
1.1 General introduction	1
1.2 Problem statement	3
1.3 The aim of the study	4
1.4 Research questions	4
1.5 The sub-objectives	4
Chapter 2- Literature Review	
2.1 Introduction	6
2.2 Gold Nanoparticles	7
2.3 Silver Nanoparticles	11
2.4 Preparation	14
2.5 Libyan flora	16
2.5.1 <i>Pistacia atlantica</i> (Anacardiaceae)	17
2.5.2 <i>Pituranthos tortuosus</i> (Apiaceae)	18
2.5.3 <i>Artemisia absinthium</i> (Asteraceae)	18
2.5.4 <i>Artemisia herba-alba</i> (Asteraceae)	18
2.5.5 <i>Helichrysum stoechas</i> (Asteraceae)	19
2.5.6 <i>Juniperus phoenicea</i> (Cupressaceae)	19
2.5.7 <i>Globularia alypum</i> ( Globulariaceae)	19

2.5.8 <i>Ajuga iva</i> (Lamiaceae)	20
2.5.9 <i>Rosmarinus officinalis</i> (Lamiaceae)	20
2.5.10 <i>Cymbopogon schoenanthus</i> (Poaceae)	21
2.5.11 <i>Peganum harmala</i> (Zygophyllaceae)	21
2.6 Oral Diseases	21
2.7 Tooth Decay	22
2.8 <i>Streptococcus mutans</i>	22
Chapter 3: Materials and Methods	
3.1 Materials and Instruments	24
3.2 Plant collection and extract preparation	25
3.3 Biosynthesis of the gold/silver nanoparticles (Au/Ag NPs)	29
3.4 Characterization techniques	
3.4.1 UV visible spectroscopy	29
3.4.2 Dynamic light scattering (DLS) Analysis	30
3.4.3 High resolution transmission electron microscopy (HR-TEM) and energy dispersive X-ray spectroscopy (EDS) analysis	30
3.4.4 X- ray diffractometer (XRD)	30
3.5 Stability analysis	30
3.6 Antibacterial evaluation	31
Chapter 4- Results and Discussion	
4.1 Determination of the optimum concentration	33
4.2 Characterisation of the biosynthesized nanoparticles	35
4.2.1 UV–vis. spectrophotometric analysis	35
4.2.2 Dynamic light scattering analysis	39
4.2.3 High resolution transmission electron microscopy (HR-TEM ) analysis	43
4.2.4 Stability assay	51
4.3 Selection of the effective plant extracts	54
4.3.1 X-ray diffraction (XRD)	54
4.3.2 Kinetic study	54
4.3.3 Evaluation of antimicrobial activity of the NPs	56
Chapter 5 - Conclusion and Future Prospects	60
References	65

# LIST OF FIGURES

<b>Figure 2.1</b> Chemical structures of mangiferin and epigallocatechin gallate.	10
<b>Figure 2.2:</b> Libyan map / <a href="https://ar.wikipedia.org">https://ar.wikipedia.org</a> .	17
<b>Figure 3.1:</b> Aerial parts of the selected plant species.	28
<b>Figure 4.1:</b> The screening of the selected plant extracts to biosynthesis gold NPs at 25 °C and 70 °C.	34
<b>Figure 4.2:</b> The screening of the selected plant extracts to biosynthesis silver NPs at 25 °C and 70 °C.	34
<b>Figure 4.3:</b> Comparison of the UV spectra of Au NPs produced at 25 (green curves) and 70 °C (red curves).	37
<b>Figure 4.4:</b> Comparison of the UV spectra of Ag NPs produced at 25 (green curves) and 70 °C (red curves).	38
<b>Figure 4.5:</b> TEM images of the synthesised Au NPs at (25°C and 70°C), the red arrow shows the halo.	45
<b>Figure 4.6:</b> TEM images of the synthesised Ag NPs at (25 °C and 70 °C).	48
<b>Figure 4.7:</b> EDS spectra of some Au NPs synthesized from A ( <i>P. atlantica</i> at 25 °C) and B ( <i>P. atlantica</i> at 70 °C) showing Au peaks in red arrows.	49
<b>Figure 4.8:</b> EDS spectra of Ag NPs synthesized from C ( <i>R. officinalis</i> at 25 °C) and D ( <i>J. phoenicea</i> , at 70 °C) showing Ag peaks in red arrows.	50
<b>Figure 4.9:</b> Stability assay of the Au NPs observed from UV-vis spectra after 24 h. upon incubation with nutrient broth media.	52
<b>Figure 4.10:</b> Stability assay of the Ag NPs observed from UV-vis spectra after 24 h. upon incubation with nutrient broth media.	53
<b>Figure 4.11:</b> Kinetic study of Au NPs using (A) <i>P. atlantica</i> , (B) <i>R. officinalis</i> and (c) $\lambda_{\max}$ values versus time.	55
<b>Figure 4.12:</b> Kinetic study of Ag NPs via (A) <i>J. phoenicea</i> , (B) <i>R. officinalis</i> and (c) $\lambda_{\max}$ values versus time.	55
<b>Figure 4.13:</b> Antibacterial activity of <i>P. atlantica</i> and its Au NPs, MIC were represented by red color determined during 24 h. Neomycin (yellow) was used as positive control.	57

**Figure 4.14:** Antibacterial activity of *J. phoenicea* and its Au, Ag NPs, MIC were represented by red color determined during 24 h. Neomycin (yellow) was used as positive control. 58

**Figure 4.15:** Antibacterial activity of *R. officinalis* and its Ag NPs, MIC were represented by red color determined during 24 h. incubation. Neomycin (yellow) was used as positive control. 59

# LIST OF TABLES

<b>Table 3.1:</b> List of the collected plant species from the Green Mountain area “Libya”	26
<b>Table 4.1.</b> The optimum concentration (OC), particle diameter (PD), polydispersity index (Pdi), $\lambda_{\max}$ and average zeta potential values (ZP) of the Au NPs synthesised from the tested plant extracts at 25 °C and 70 °C.	41
<b>Table 4.2.</b> The optimum concentration (OC), particle diameter (PD), polydispersity index (Pdi), $\lambda_{\max}$ and average zeta potential values (ZP) of the Ag NPs synthesized from the tested plants at 25 °C and 70 °C.	42



# Chapter 1

## INTRODUCTION

### 1.1 General introduction

The last century has witnessed the progress of the pharmaceutical industry, and many drugs have been introduced to treat different human diseases. Although there have been many improvements in human disease treatments and drug discovery, there are grave diseases like cancer and HIV, which are still quite difficult to treat. The uncontrolled use and drug delivery resulted in harmful side and toxic effects due to powerful and toxic drugs being released too quickly [Park et al., 2015]. There is considerable evidence from recent studies supporting positive correlations between the uncontrolled drug use and many humans associated diseases. Additionally, many drug resistant diseases have been generated due to the excessive use of antibiotics [Swain et al., 2014].

Green bio-economy based strategies have been initiated in the last century to counter the negative effects of chemical pollutions and their adverse effects on human health as well as the environment. Consequently, and as a result of tremendous chemical (including pharmaceutical) pollutions, the green chemistry concept has been implemented. The green chemistry dedicated to design new effective, safe, and innovative chemicals (drugs) without harming the environment and protect the economy growth.

Nanotechnology has emerged as an elementary division of modern science and stemmed directly from green chemistry twelve basic concepts, it received global attention due to its unique character and ample applications. They also have great potential to mitigate the challenges they face in various scientific fields such as the medical, fuel and energy sectors [Cele et al., 2015]. The notable development of nanotechnology in recent years, new approaches for drug design based on the state-of-the-art nanotechnology have been receiving significant attention. Nanodrugs are increasingly considered as a potential candidate to carry therapeutic agents safely into a targeted compartment in an organ, particular tissue or cell.

Different NPs have been introduced using polymers, metals, and ceramics, and according to their manufacturing methods and materials, these particles can take various shapes and sizes with distinct properties.

Metallic nanoparticles, especially noble metals such as silver and gold have been developed and reported to have interesting applications including in different medical fields [Isaac et al. 2014]. Various physical and chemical methods have been employed to synthesize metal nanomaterials [Akhtar et al., 2013; Iravani et al., 2014]. These methods are expensive and include the use of many toxic and harmful chemicals to the environment and living organisms. Thus, there is an obvious need for an alternative, cost-effective and at the same time safe and environmentally friendly routes toward the manufacturing nanomaterials [Lukman et al., 2011].

In recent years, there has been growing interest in the green synthesis of nanoparticles, through applications of biological natural resources, using biotechnology tools that are considered safe and environmentally sound as an alternative to conventional chemical methods. This has led to the concept of green nanotechnology [Joerger et al., 2000]. In general, this technique means the synthesis of nanomaterials using biological methods involving microorganisms, plants, viruses. The principles of green nanotechnology are now a reference and guide for researchers and scientists around the world as a basic section of modern science for the development of less dangerous techniques and a new era in the field of materials science and are gaining international attention because of their extensive applications [Parashar et al., 2009].

Green synthesis of nanoparticles using aqueous plant extracts seems to be a very effective method in developing a rapid, clean, nontoxic, and eco-friendly technology. The use of plant biomass or extracts for the biosynthesis of novel metal nanoparticles from silver and gold would be more significant if the nanoparticles are synthesized in a controlled manner according to their shape and size. It is also a very rapid and cost-effective approach that can be easily scaled up for bulk production of nanoparticles [Akhtar et al., 2013; Shankar et al., 2004; Iravania et al., 2011]. Owing to the rich biodiversity of plants, their potential use toward the synthesis of these noble metal (gold and silver) nanoparticles is yet to be explored. However, their potential is still not fully utilized for the manufacture of green metal nanoparticles.

The flora of Libya can be distinguished by regions, the Mediterranean, the semi-desert and the desert regions. The Mediterranean coast of Libya is characterized by its rich biodiversity with strong links to the eastern Mediterranean region (Palestine to Greece). Despite the immense development of the pharmaceutical industry, large populations in the world including some desert areas in Libya rely on medicinal plants for diseases treatment.

Libya is a vast desert country with a vast wealth of medicinal plants linked to a popular medical heritage developed by the evolution of civilizations [Radford et al. 2011].

## **1.2 Problem statement**

The expected effect of nanomaterials on human health is remarkable. However, nanoparticles (NPs) can also have harmful effects on the environment.

The unique behavior of nanomaterials is directly related to its small sizes and high surface to mass ratio. The advantage of such tiny materials is their capability to penetrate the cell surface and produce biological effects. However, there is a high risk of nano-pollutants from the uncontrolled use and emission of NPs. These nanopollutants, together with the use of toxic compounds, as capping materials, are chemically active and can easily interfere with the biological system and cause unexpected environmental problems. In addition, the conventional methods used for preparation of NPs (e.g. gold/silver) involve many virulent chemicals, which can cause direct harm to the environment. This project is designed to screen selected Libyan medicinal plant extracts to synthesize gold and silver nanoparticles, which will nontoxic and biocompatible with nature.

There are a wide range of innovative biological applications of NPs in diagnosis, treatment of illnesses and drug delivery. Hence, the search for biocompatible and toxin-free NPs is mandatory for future applications of these materials in nanomedicine. The natural bioactive compounds under consideration in this project (according to the literature review) are safe and proved to be multifunctional and multi-therapeutics as well.

The current uncontrolled use of drugs causes many side effects including drug resistance phenomena (e.g. antibiotics resistive bacteria, some resistive cancers) as well as polluting the environment. Effective multifunctional and biocompatible drugs are therefore required to decrease such resistivity. This project will study in detail the possibility to merge multifunctional bioactive natural products to prepare NPs for effective antibacterial treatment.

### 1.3 The aim of the Study

The main aim of this study is to explore the potential of selected Libyan medicinal plants as effective source(s) for synthesizing biocompatible gold and silver NPs and to test the antibacterial activity of the most stable NPs.

### 1.4 Research questions

- a) What are the possibilities of synthesizing nanoparticles from the selected plant extracts?
- b) Is the use of plant extracts effective as an eco-friendly method for the synthesis of NPs?
- c) What is the effect of temperature change on the synthesis of the nanoparticles?
- d) Will the resultant NPs be stable in biological media?
- e) Will the resultant NPs and their plant extracts have any antibacterial activity against *S. mutans*?

### 1.5 The sub-objectives

- a. Collection of samples of the selected plants from their natural environments and identification, documentation by taxonomist.
- b. Preparation of the plant extracts.
- c. Screening of the extracts for the possibility of the synthesis nanoparticles (Au/Ag NPs).
- d. Study the effect of temperature on the synthesis of NPs.
- e. Assessing the stability of the NPs, and select the most stable ones.
- f. Evaluate the antibacterial activity of synthesized NPs against *S. mutans* “the etiological agent of dental caries”.



# Chapter 2

## Literature Review

### 2.1 Introduction

The field of nanotechnology introduced new materials with new dimensions and different properties as compared to their larger counterparts and this can be attributed to their high surface-to-volume ratio. Due to these unique properties, they make excellent candidates for biomedical applications as a variety of biological processes occur at nanometer scale. The wide range of applications reported for different nanoparticles indicated a significant impact on the industrial sector as well as society. Recently, different applications for nanotechnology have been reported in different fields such as electronic storage systems, magnetic separation and preconcentration of target analytes, targeted drug delivery, and vehicles for gene and drug delivery [Rudge et al., 2001; Kang et al., 1996; Appenzeller 1991].

The size range of nanoparticles used in the field of biotechnology vary mainly between 10 and 500 nm. These nanosize entities generate possible communications with different biomolecules on the cell surfaces and within the cells in ways that can be decoded and designated to various biochemical and physiochemical properties of these cells. Similarly, its potential application in drug delivery systems and noninvasive imaging offered various advantages over conventional pharmaceutical agents [Mody et al., 2009].

For medical applications the NPs should be:

- 1- Stable, biocompatible, and nontoxic,
- 2- Selective to specific biological sites,
- 3- Conjugate with different ligands with specific binding activity,
- 4- Attach to therapeutic substances to increase the concentration at the pathological site.

Metallic nanoparticles such as gold and silver have shown great potential as diagnostic and therapeutic agents and there are many scientific reports supporting their power and efficiency. Metallic nanoparticles (MNPs) have found significant utility over a diverse spectrum of biomedical activities such as imaging, sensing, and therapeutics. They have provided an invaluable advance in the detection, diagnosis, and therapy of different human cancers and this has led to the development of a completely new discipline, nano-oncology. Colloids of gold,

silver, platinum, and palladium have been widely used and accepted in clinical trials for treatment of cancer. Nanostructures have attracted considerable interest as theranostic agents, but their pharmacokinetics, biodistribution, side effects, and safety profile within the human body, need more thorough investigation for future applications [Ackerson et al., 2005; Roux et al., 2005; Wilton-Ely 2008].

The antibacterial, antifungal, antiviral, and antimicrobial properties of plasmonic nanomaterials are already well established and this could be a future strategic approach for the design and development of nanodrugs in the pharmaceutical industries. Toxicological studies based on numerous nanocomposites have provided sufficient data regarding their non-toxicity, but possible toxic side effects upon incorporation into the human body cannot be ruled out completely. The biocompatibility issue related to nanomaterials can be addressed by considering the dose of nanoparticles and the surface modulation. These two aspects in conjunction provide a reliable and sufficient approach to the use of nanomaterials in clinical applications.

It is of utmost importance to test nanoparticles and biological interactions in order to modify the nanostructures for optimal biocompatibility and thereby prevent damage to healthy tissues. In addition, the incorporation of MNPs in diagnostic and detection devices is likely to grow, as the translation of these devices are much less complicated than *in vivo* therapeutic applications. At the same time, more advanced diagnostic devices can be created with the help of MNPs. There are other lesser known MNPs such as Rh, Ru, Ir, and Os nanocomposites, whose diagnostic, sensing, and therapeutic abilities need to be understood in more detail and there is still much work to be done in the area to realise the full benefits of nanobiotechnology in the field of healthcare and environmental preservation.

## **2.2 Gold Nanoparticles**

In the 1850 Michael Faraday observed that the colloidal gold solutions have properties that differ from the bulk gold especially when it comes in contact with the light [Hayat 1989]. The colloidal solution with size less than 100 nm has an intense red color while larger sizes show a dirty yellowish color [Murphy et al., 2008]. These unique interactions with light resulted in the localized surface plasmon resonance which after absorption of the light can be transformed into heat.

Au NPs have the advantage of ease of functionalization with therapeutic agents through covalent and ionic binding. Combining Au NPs and other materials can result in nanoplatforms, which can be useful for biomedical applications. Biomaterials such as biomolecules, polymers and proteins can improve the therapeutic properties of nanoparticles, for examples, Serum albumin is a versatile, non-toxic, stable, and biodegradable protein, in which structural domains and functional groups allow the binding and capping of inorganic nanoparticles. Au NPs coated with albumin have improved properties such as greater compatibility, bioavailability, longer circulation times, lower toxicity, and selective bioaccumulation [Bolanos et al., 2019].

Au NPs were prepared using individual amino acids such as glutamic acid, phenylalanine and tryptophan with optimum concentration of amino acids (25 mM). The size of nanoparticles obtained were 5–20, 10–20 and 20–30 nm, respectively. The results obtained from experimental and quantum calculations confirmed that amino acids have strong bonds. Amino acids have an advantage over other compounds for containing both basic and acidic groups in the same molecules this advantage give strong interactions with the Au NPs surface and also can be used to bind other bioactive compounds to the surface [Zare et al., 2014].

The conjugation of Au NPs with arginine–glycine–aspartic acid peptide (RGD) and a nuclear localization signal peptide (NLS) were studied in-vitro against human oral squamous cell carcinoma. RGD is known to target  $\alpha_v\beta_6$  integrins receptors on the surface of the cell, whereas NLS sequence lysine–lysine–lysine–arginine–lysine sequence is known to associate with karyopherins (importins) in the cytoplasm, which enables the translocation to the nucleus. The results showed that the RGD-Au NPs specifically target the cytoplasm of cancer cells over that of normal cells, and the RGD/NLS-Au NPs specifically target the nuclei of cancer cells over those of normal cells [Makey et al., 2010].

Au NPs have emerged as a therapeutic agent, and are useful for imaging, drug delivery, and photodynamic and photothermal therapy. The properties and applications of Au NPs depend upon its shape, and size and due to these unique optical properties. Gold nanoparticles are the subject of substantial research, with enormous applications including biological imaging, electronics, and materials science [Rao et al., 2000].

Photothermal therapy (PTT) is a procedure in which a photosensitizer is excited with specific band light (mainly IR). This activation brings the sensitizer to an excited state where it then releases vibrational energy in the form of heat. The heat is the actual method of therapy that kills the targeted cells. One of the biggest recent successes in photothermal therapy is the use

of gold nanoparticles. PTT of Au NPs <5 nm coated with Bovine Serum Albumin (BSA) was tested against three types of cancer cell lines; Rhabdomyosarcoma, Murine fibroblast and RAW 264.7 monocyte-macrophage at different concentration using low power laser irradiation, green (532 nm) and near-infrared (NIR) (800 nm) at 0.5, 1, 2 and 3 min, separately. Prominent results were demonstrated in the green and NIR region by pH -induced aggregation effect of small nanoparticles inside the cancer cells, which make the small-sized BSA-Au NPs are promising agents for cancer photothermal therapy [Al-Jawad et al., 2018].

Resveratrol was used as reducing and capping agents for the synthesis of Au NPs. Increasing the payload of resveratrol to threefold increased in the anti-cancer effects with optimal cellular uptake after 24-hour incubation. A synergistic approach facilitated by gum Arabic increased the overall stability and provided a protein matrix support for enhanced resveratrol loading onto the surface of the Au NPs [Thipe et al., 2019].

Radiolabeling is a well-known technique for assessment of the biological uptake and pharmacokinetics of synthetic nanomaterials. Several  $\gamma$ -ray-emitting radionuclides including positron emitters ( $\beta^+$  decay) have been extensively used for developing nanomaterial-based diagnostic agents [Geol et al., 2017]. These radiolabelled NPs can be used to visualize tumor tissues in living subjects as well as other important biological phenomena. Gold-198 is a typical  $\beta$ -ray-emitting radioisotopes with reasonable half-life ( $^{198}\text{Au}$ ,  $t_{1/2}=2.70$  days). Also, it is available and can be produced easily from its  $^{197}\text{Au}$  isotope.

Gold-198 has a  $\beta$  decay energy of 0.960 MeV. Its average penetration depth in tissue is sufficient to provide therapeutic effects to destroy tumor cells. Gold NPs in general and especially the  $^{198}\text{Au}$  isotope, have favourable physicochemical properties, and attracted interest for the radiotherapy research in cancer fields. The core-shell nanostructure silica-coated  $^{198}\text{Au}$  NPs was prepared using neutrons in a nuclear reactor, and was stable [Jung et al., 2010].

Mangiferin is a bioactive compound distributed in many natural sources especially mango and honey bush. The compound was used as reducing and stabilizing agent to prepare  $^{198}\text{Au}$  NPs. The laminin receptor specificity of mangiferin affords specific accumulation of therapeutic payloads of this new therapeutic agent within the prostate tumors. The intratumoral delivery of MGF- $^{198}\text{Au}$  NPs, show the retention of over 80% of the injected dose (ID) in prostate tumors up to 24 h. By three weeks post treatment, tumor volumes of the treated group of animals showed an over 5-fold reduction as compared to the control saline group [Al-Yasiri et al., 2017].

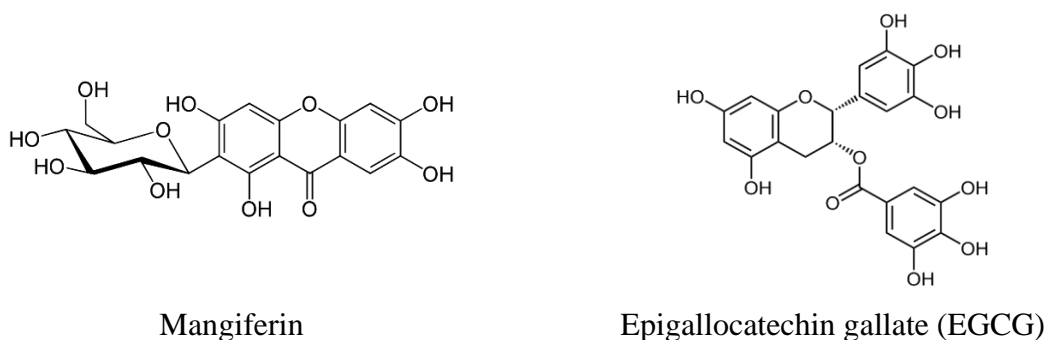


Figure 2.1, Chemical structures of mangiferin and epigallocatechin gallate

Another study by the same group, using epigallocatechin gallate,  $^{198}\text{Au}$  NPs produced and showed a selective binding with excellent affinity to Laminin67R receptors, which are over expressed in prostate tumour cells. The studies showed 80% reduction of tumor volumes after 28 days demonstrating significant inhibition of tumor growth compared to controls [Khoobchandani et al., 2016].

Intratumoral injection of gold nanoparticles coated with EGCG can achieve a favorable gold distribution, namely high gold retention in tumor site and low gold leakage into normal tissues, leading to pronounced tumor inhibition without perceived host toxicity. Accordingly, EGCG, as an FDA-approved phytochemical for application in humans, has the potential to be employed for fabricating other therapeutic payloads for targeted delivery.

Animal studies on Au NPs have shown that gold nanoparticles modified with certain thiol monolayers such as tiopronin can cause renal complications and morbidity. Although these effects may be eliminated by coadsorbing small amounts of polyethylene glycol (PEG) onto the nanoparticle surface, PEG can also lower cellular internalization efficiency and binding interactions with protein disease targets, significantly reducing the potential for using Au NPs as therapeutics. On the other hand, glutathione-coated Au NPs ( $1.2 \text{ nm} \pm 0.9 \text{ nm}$ ) cause no morbidity at any concentration up to and including  $60 \mu\text{M}$  and target primary organs although providing gradual dissipation and clearance over time. This study suggests that glutathione may be an attractive alternative to PEG in the design of Au NPs therapeutics [Simpson et al., 2013].

### 2.3 Silver Nanoparticles

Like gold nanoparticles, silver has a long history and was initially used to stain glass yellow. Currently, there is also an effort to incorporate Ag NPs into a wide range of medical

devices, including bone cement, surgical instruments, and surgical masks. Moreover, it has also been shown that ionic silver, in the right quantities, is suitable in treating wounds [Atiyeh et al., 2007]. Due to their attractive physiochemical properties these nanomaterials have received considerable attention in biomedical imaging using SERS. In fact, the surface plasmon resonance and large effective scattering cross-section of individual silver nanoparticles make them ideal candidates for molecular labelling [Schultz et al 2000].

The interesting property of the noble metals is a promise that they would be continuously used as newer applications and protocols are being developed. Silver nanoparticles possess anticancer and antitumour properties by inhibiting angiogenesis around tumour tissues. This has led to extensive research regarding the potential application of Ag NPs in cancer treatment both *in vitro* and *in vivo*. These studies have been conducted on different cancerous cell line models such as MCF-7, B10F17, A549, SiHa, and HeLa cell lines.

Ag NPs were synthesized using the leaf extracts of *Cynara scolymus* (Artichoke) applying microwave irradiation. The anti-cancer potential with photodynamic therapy (PDT) was evaluated against MCF7 breast cancer cells using MTT assay. Mitochondrial damage and intracellular reactive oxygen species (ROS) production were observed upon treatment with Ag NPs (10 µg/mL) and PDT (0.5 mJ/cm<sup>2</sup>) showed significant reduction in cell migration, expression of Bax and suppression of Bcl-2. Significantly, biosynthesized Ag NPs showed a broad-spectrum anti-cancer activity with PDT therapy and therefore represent promoting ROS generation by modulating mitochondrial apoptosis induction in MCF7 breast cancer cells [Erdogan et al., 2019].

In another study, the aqueous extract of *Nepeta deflersiana* was used to synthesize Ag NPs. The anticancer potential of the Ag NPs were investigated against human cervical cancer cells (HeLa) using MTT, neutral red uptake (NRU) assays, and morphological changes. The concentration-dependent cytotoxic effect was observed with a significant increase in ROS and lipid peroxidation (LPO), along with a decrease in MMP and glutathione (GSH) levels. The cell cycle analysis and apoptosis/necrosis assay data exhibited Ag NPs-induced SubG1 arrest and apoptotic/necrotic cell death [Al-Sheddi et al., 2018].

Using *Anthemis atropatana* extract, Ag NPs were synthesized and evaluated for its anticancer activity against colon cancer cell lines (HT29) using MTT assay. The Ag NPs had maximum cytotoxicity on HT29 cancer cell line at 100 µg/mL concentration, the real time PCR

and flow cytometry results confirmed the apoptotic effects of Ag NPs [Dehghanizade et al., 2017].

The synergistic cytotoxic effects of a curcumin derivative and Ag NPs was studied. The Ag NPs were synthesized using a curcumin derivative, ST06. The synthesized nanoparticles ST06-Ag NPs were assessed *in vitro* for its cytotoxic effects by MTT assay and showed significant growth inhibition of human cervical cancer cell line (HeLa). In addition, *in vivo* studies carried out in EAC tumor-induced mouse model (Ehrlich Ascites carcinoma) using ST06-Ag NPs, revealed that treatment of the animals with these nanoparticles resulted in a significant reduction in the tumor growth, compared to the control group animals. The tumor suppression is associated with the intrinsic apoptotic pathway. Together, the results of this study suggest that ST06-Ag NPs could be considered as a potential option for the treatment of solid tumors [Murugesan et al., 2019].

The Ag NPs synthesized using aqueous latex extract of *Euphorbia antiquorum* L exhibited significant antimicrobial and larvicidal activity against bacterial human pathogens as well as disease transmitting blood sucking parasites such as *Culex quinquefasciatus* and *Aedes aegypti* (3<sup>rd</sup> instar larvae). Additionally, the Ag NPs has shown potential anticancer activity against human cervical carcinoma cells (HeLa) at  $IC_{50} = 28 \mu\text{g/mL}$  [Rajkuberan et al., 2017].

The anti-aging effect of Ag NPs synthesized using *Symphytum officinale* leaf extract were investigated in HaCaT keratinocyte cells. The Ag NPs significantly inhibited the production of matrix metalloproteinase-1 and IL-6 but increased the expression of procollagen type 1. The data suggest that Ag NPs have photoprotective properties and may have potential to be used as an agent against photoaging [Singh et al., 2018].

Recently, increased ROS levels and altered redox status in cancer cells have become a novel therapeutic strategy to improve cancer selectivity over normal cells. Ag NPs display anti-leukemic activity via ROS overproduction, and it can improve therapeutic efficacy of ROS-generating agents against leukemia cells. Ag NPs synthesized by N-(4-hydroxyphenyl)retinamide (4-HPR), a synthetic retinoid, was used as a drug model of ROS induction to investigate its synergistic effect with Ag NPs. The combination of Ag NPs together with 4-HPR as capping agent showed more cytotoxicity and apoptosis via overproduction of ROS in comparison with that alone. As a result, Ag NPs combined with ROS-generating drugs could potentially enhance therapeutic efficacy against leukemia cells, thereby providing a novel strategy for Ag NPs in leukemia therapy [Guo et al., 2015].

Monomeric polymer encapsulated Ag NPs have shown antileukemic properties against AML human cell lines in a dose and size dependent manner. The Ag NPs induce apoptosis and DNA damage through the production of ROS and release of silver ions (Ag) from nanomaterials. The production of ROS by Ag ions is pH dependant (only acidic) and confers their anticancer and antitumour activity [Ge et al., 2013].

The synthesis of Ag NPs using leaf extract of *Podophyllum hexandrum* Royle and their effects against human cervical carcinoma cells by MTT Assay, The overall result indicates that Ag NPs can selectively inhibit the cellular mechanism of HeLa by DNA damage and caspase mediated cell death [Jeyaraj et al., 2013].

Halloysite Nanotubes (HNTs) are aluminosilicate clay-based nanotubes which are abundant in nature. The multilayer hollow tubular structure of HNTs results from the wrapping of the 1:1 aluminosilicate clay mineral sheets under specific geological conditions. Al, Si, H, and O are the four main elements which formulated the composition of these clay-based nanotubes [Saif et al., 2018].

Recently, incorporation of HNTs with various antimicrobial agents as interfacial materials between these nanotubes and pathogenic microorganisms, for the development of antimicrobial nanocomposites with enhanced antimicrobial activities has gained researcher's interest. Metal nanoparticles including Ag NPs with HNTs have been used for the synthesis of antimicrobial nanocomposites.

In another study, surface modified HNTs with silver nanoparticles (Ag NPs) as an interface between these nanotubes and bacterial cells exhibited an inhibition zone of 19.2 mm against *E. coli*, indicating their excellent antibacterial behavior. The mechanism of antibacterial activities of Ag NPs may be due to the attachment of Ag NPs to the membrane of microorganism and destruction of the cell membrane [Song et al., 2019].

## **2.4 Preparation**

The most prevalent method for the synthesis of monodisperse spherical gold nanoparticles was pioneered by Turkevich et al. in 1951 and later refined by Frens et al. in 1972. This method uses the chemical reduction of gold salts such as hydrogen tetrachloroaurate (HAuCl<sub>4</sub>) using citrate as the reducing agent. This method produces monodisperse spherical gold nanoparticles in the range of 10–20 nm in diameter. However, the synthesis of larger Au

NPs with diameters between 30 and 100 nm was reported by Brown and Natan *via* seeding of Au<sup>3+</sup> by hydroxylamine [Brown & Natan 1998]. Subsequent research led to the modification of the shape of these Au NPs resulting in rod, triangular, polygonal rods, and spherical particles [Jana et al., 2001a; 2001b; Subrata et al., 2007]. These ensuing Au NPs have unique properties, providing a high surface area to volume ratio. Moreover, the gold surface offers a unique opportunity to conjugate ligands such as oligonucleotides, proteins, and antibodies containing functional groups such as thiols, mercaptans, phosphines, and amines, which demonstrates a strong affinity for gold surface [Alivisatos et al., 1996]. The realization of such gold nanoconjugates coupled with strongly enhanced LSPR gold nanoparticles have found applications in simpler but much powerful imaging techniques such as dark-field imaging, SERS, and optical imaging for the diagnosis of various disease states [El-Sayed et al., 2005].

The preparation of nanoparticles follows two different strategies, top-down and bottom-up. The top-down processes involve bulk materials which are reduced to particles with nano-dimension using various physical and chemical methodologies. On the other hand, in a bottom-up approach, nanoparticles are constructed through the assembly of the atoms, the molecules, or the clusters and thus this is generically termed self-assembly. The most commonly utilised and easiest bottom-up approach is the chemical reduction of metal ions in solutions. In principle, an ionic salt is reduced using various reducing agents under appropriate reaction conditions and in presence of a stabilising agent [Schulz-Dobrick et al., 2005; Liu et al., 2017].

A plethora of reducing agents, such as Na-citrate, hydrazine, hydrogen, LiAlH<sub>4</sub>, NaBH<sub>4</sub>, and alcohols can be used. According to the Lee–Meisel method, nitrate and sulphate salts are reduced using NaBH<sub>4</sub>, sodium citrate, and hydrogen. The pH of the medium plays a crucial role in modulating the size and shape of the particles [Dong et al., 2009; Lee and Meisel 1982].

At high pH, owing to faster reduction, both rod and spherical nanoparticles were found, while at relatively lower pH triangular and other polyhedral structures were obtained because of the slower reaction [Sanvicens & Marco, 2008].

Similarly, Au NPs can be prepared from an aqueous solution of HAuCl<sub>4</sub> using citrate as the reducing agent. The average particle size can be controlled by varying the ratio of reducing/stabilising agents as well as the pH of the system. Another popular nanoparticle fabrication process involves microemulsions. The process gained popularity owing to its ease of operation and control over the size and shape of the products, where, two separate

microemulsions containing salts and reducing agents are mixed together in presence of amphiphile. This method offers benefits to prepare thermodynamically stable and monodispersed nanoparticles [Holmberg 2003].

Importantly, control over the particle size can easily be achieved without any template. Considering the excess use of chemicals and solvents in the chemical synthesis of nanoparticles, greener approaches with minimal use of such hazardous chemicals have been developed. One major driving force for these greener approaches is nature's efficiency in making these nano-materials. Mimicking nature, may not be not easy, but it has allowed chemists to develop several green synthetic protocols for nanoparticle synthesis using water as the medium and proteins or carbohydrates as capping agents. Starch has been used as both a reducing and stabilizing agents as well [Dahl et al., 2007; Raveendran et al., 2003].

The nature of engineered nanomaterials and their proposed uses provides compelling reasons for the implementation of green chemistry in the development of the new materials and applications. The technology is early in development and expected to be widely applied and distributed.

Traditional medicinal plants have been used as medical treatments for many diseases for thousands of years in many countries of the world. The use of medicinal plants in the pharmaceutical field has increased significantly and many researchers in this field have focused their research on the study of these plants which are spread around the world. Medicinal plants are used for various therapeutic purposes. Medicinal plants contain various compounds that have different roles in a biological system including plant protection from diseases. These compounds showed potential for treatment of human pathologies related to pathogenic microorganisms. Additionally, and in the last few years, aqueous extracts from a couple of hundreds plant materials were used successfully for the preparations of different metal NPs, the previous sections included some examples. The advantage of the use of medicinal plant extract is the safety for medical applications which can't be offered using harsh chemicals.

## **2.5 Libyan flora**

Libya is located in the northern part of Africa and occupies an area of about 1.7 million square kilometres, (mostly desert). The most important areas for plant diversity are the coastal strip and the mountains of the Mediterranean coast (1900 km). The Mediterranean coast of

Libya is characterized by its rich biodiversity. The region of the Green Mountain contains about 50% of the natural plants throughout the country. Plants are predominantly Mediterranean, with stronger links to the eastern Mediterranean (Palestine to Greece) than the rest of North Africa., and the island of Crete [Radford et al., 2011; Boulos 1971]. Libyan medicinal plants are used largely in traditional medicine for the treatment of different diseases. Some of the important Libyan medicinal plants selected under this study listed below with the chemical and pharmacological importance.

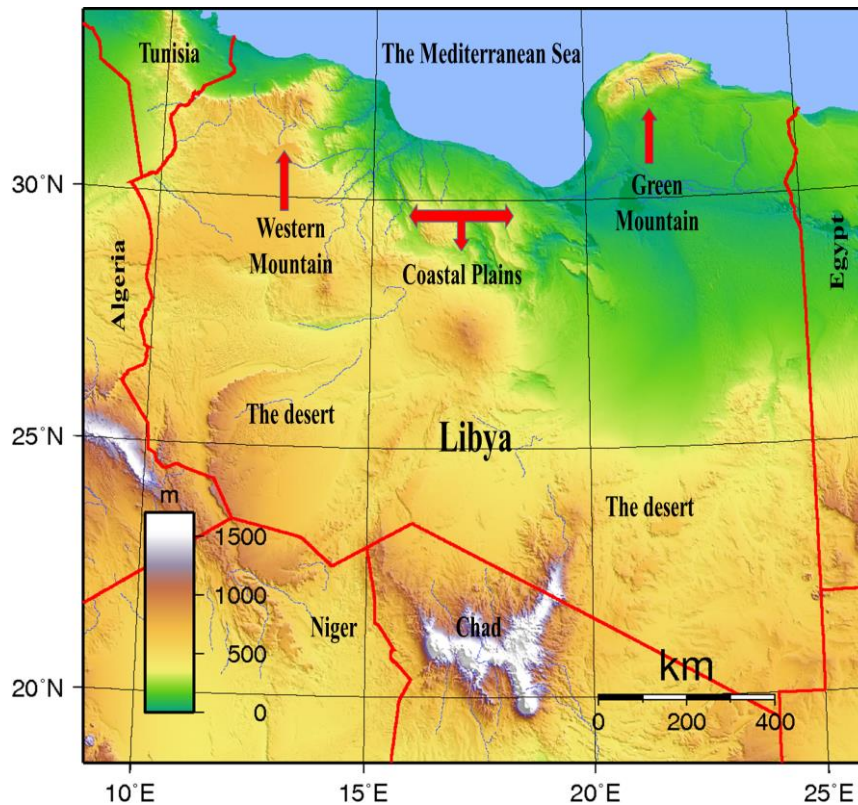


**Figure 2.2:** Libyan map / <https://ar.wikipedia.org>

### 2.5.1 *Pistacia atlantica* (Anacardiaceae)

*Pistacia atlantica* is a well-known herbal medicine in the Middle Eastern and Mediterranean areas and used traditionally for stomach diseases, renal disorders, wounds and coughs. The plant showed different pharmacological



properties such as antioxidant, antidiabetic, antihyperlipidemic, anti-inflammatory, anti-cancer, antibacterial. The plant contains triterpenes (oleanolic, ursonic, masticadienonic, masticadienolic, morolic, and 3-*O*-acetyl-3-epiisomasticadienolic acids), phenolic such as

gallic acid and gallic acid methyl ester, luteolin, luteolin 7-glycoside, chlorogenic acid, kaempferol, naringin and naringin 7-glucoside, kaempferol-3-*O*-glucoside, quercetin-3-glucoside, quercetin-3-galactoside, quercetin-3-rutinoside, quercetin-3-glucoside-7-*O*-galactoside, vicenin 2 [Bagheri et al. 2019; Mahjoub et al. 2018; Amri et al. 2018; Hajjaj et al. 2018;]. The aqueous extract was reported for preparation of different NPs such as Ag NPS, Ag<sub>2</sub>S NPs, Pd NPs, Au NPs. [Zahedifar et al., 2019; Hamedani 2019].

### 2.5.2 *Pituranthos tortuosus* (Apiaceae)

*Pituranthos tortuosus* (Coss.) Maire (Apiaceae), grows naturally in North Africa, the plant is used traditionally to relief stomach pains, against intestinal parasites, when blood is excreted in the urine or when coughing blood, and for the regulation of menstruation for asthma and against scorpion's stings. The plant contains furanocoumarins [Mighri et al. 2015; Abdel-Kader 2003].



### 2.5.3 *Artemisia absinthium* (Asteraceae)

*Artemisia absinthium* Linn (Asteraceae family) is an aromatic, bitter, shrubby plant. The aerial parts used traditionally as anti-helminthic, and intermittent for digestive problems. It exhibits various pharmacological activities such as anthelmintic, stomachic, diabetes, liver tonic and anti-inflammatory, and antidote of insects bite. The plant contains different constituents such as essential oil rich in thujone and thujole, flavonoids, sesquiterpenes, amino, fatty, and organic acids and tannins [Ashraf et al., 2019; Abdullah et al., 2018; Goud & Poornima 2018]. The plant extract was used to generate Ag NPs and their antifungal activities were evaluated against different *Candida* species. [Rodriguez-Torres et al., 2019]



#### 2.5.4 *Artemisia herba-alba* (Asteraceae)

*Artemisia herba-alba*, is an important medicinal plant native to the Mediterranean area, Western Asia (Arabian Peninsula) and South-western Europe. It is widely used traditionally for diabetes, infections, worms and has antispasmodic properties, it was reported as a traditional remedy of enteritis, and various intestinal disturbances, among the Bedouins in the Negev desert. The plant extract showed hypoglycaemic, antioxidant, antimicrobial, cytotoxic activities. It contains flavonoids, coumarins, terpenoids, fatty acids, carbohydrates, organic acids and alkaloids [Aziz et al., 2018].



#### 2.5.5 *Helichrysum stoechas* (Asteraceae)

*Helichrysum stoechas* (L.) Moench is a typical Mediterranean plant growing in North Africa, traditionally has been used as an ornamental, medicinal and food plant. It showed anti-inflammatory, anti- $\alpha$ -glucosidase and anti-dipeptidyl peptidase-4, antiproliferative, antioxidant, antidiabetic and neuroprotective activities. The phytochemical analysis showed phloroglucinols, phenolic acids, flavonoids, and sesquiterpene [Silva et al., 2017; Les Francisco et al., 2017; El-Dahmy 1993].



#### 2.5.6 *Juniperus phoenicea* (Cupressaceae)

*Juniperus phoenicea* L. (The Phoenician juniper) is a Mediterranean plant growing in the North Africa and naturalized as ornamental trees. Different part of the plant used in traditional medicine to treat different diseases such as gout, arthritis and rheumatism. The plant extract showed antibacterial, antioxidants anti-inflammatory, cytotoxicity, and antidiabetic (increase insulin level) activities. The chemical constituents of the plant include flavonoids, phenolic acids, and diterpenes [Boussida et al., 2018; Hasan & Ali 2017; Al-Ahdab 2017]. The plant was used previously to synthesize Ag NPs [Maeh et al., 2019]



### **2.5.7 *Globularia alypum* ( Globulariaceae )**

*Globularia alypum* L. is a Mediterranean plant. The aqueous extract is widely used to treat various ailment including constipation, peptic ulcer, diabetes, insomnia, hernia and intestinal pain. The plant extract showed different biological activities such as Antifungal, antibacterial, antioxidant, anticoagulant and protective effect against oxonate-induced hyperuricemia and renal dysfunction. The plant contains different chemical constituents such as flavonoids, iridoids, and alkaloids [Kraza et al., 2019; Ghilissi et al., 2019; Hajjaj et al. 2018; Sertic et al., 2015].



### **2.5.8 *Ajuga iva* (Lamiaceae)**

*Ajuga iva* is an aromatic plant belong to family Lamiaceae. The plant is used extensively in traditional medicines for treatment of different diseases, it has different biological activities such antidiabetic and anti-inflammatory, [Medjeldi et al 2018; Tahraoui et al. 2017; Boudjelal et al. 2015], the plant not explored yet for the synthesis of metal nanoparticles.



### 2.5.9 *Rosmarinus officinalis* (Lamiaceae)

*Rosmarinus officinalis* (Rosemary) is a common herbal medicinal plant belong to the family Lamiaceae.

Rosemary also has been used extensively as a medicinal herb for its astringent, spasmolytic, anti-inflammatory, expectorant, carminative, antirheumatic, analgesic, antimicrobial, and hypotensive properties. The use of the rosemary leaf to treat dyspepsia, high blood pressure, and rheumatism was approved by the German Commission E at doses of 4 to 6 g/day. Other pharmacologic effects attributed to rosemary include antimutagenic, anticancer, hepatoprotective, and antioxidant activities. Some reports indicated the use of rosemary in the synthesis of silver NPs [Nancy & Elumalai. 2019; Ando et al., 2019; Velgosova & Veselovsky 2019; Arassu et al., 2018] .



### 2.5.10 *Cymbopogon schoenanthus* (Poaceae)

*Cymbopogon schoenanthus* is an aromatic plant cultivated in north Africa for its essential oil. It's very common in traditional medicine, is used as antispasmodic, anti-fever, stomachic anti-malarial, and anti-helminthic, antispasmodic, diuretic, sedative, digestive and anti-parasitic. It has antifungal and anti-inflammatory activities [Ben Othman et al., 2017; Al-Ali et al., 2017; Kadri et al., 2017; Hashim et al., 2017]. The plant extract was used recently to synthesize zinc oxide NPs [Awad et al., 2019].



### 2.5.11 *Peganum harmala* (Zygophyllaceae)

*Peganum harmala* L. is native to eastern Mediterranean region. The plant is widely distributed and used as a medicinal plant in North Africa and Middle East. The seeds used extensively in traditional medicine, for its curing properties such as



anti-inflammatory, antidiabetic, antibacterial, for skin problems, respiratory system, and tumours. The biological activities attributed to the alkaloidal content especially harmaline. [Moloudizargari et al., 2013]. The plant reported in the synthesis of different types of NPs such as Iron oxide, zinc oxide, silver, and gold [Miri et al., 2019; Moustafa Al-Omari 2019; Alomri et al., 2018; Azizi et al., 2017; Amin et al., 2014]

## 2.6 Oral Diseases

Oral diseases are major health problems representing a serious infectious disease. Oral health affects the general quality of life and is associated with poor oral health, chronic diseases and systemic diseases. More than 750 species of bacteria live in the mouth cavity and can cause a number of oral diseases. The increasing resistance of bacteria to antibiotics represents another challenges for the current treatment, and there is a need for alternative prevention and treatment options that are safe, efficacious and cost-effective [Palombo 2011].

### 2.7 Tooth Decay

Tooth decay occurs by the acid on the surface of the enamel. Acid is produced as a result of the interaction of the bacteria with different sugars in the dental biofilm (plaque) on the surface of the teeth. Acid production leads to loss of calcium and phosphate from the enamel. With inappropriate health hygiene this can lead to a cavity, and subsequently weaken the teeth and many inflammation problems. [Featherstone, 1999]

### 2.8 *Streptococcus mutans*

*Streptococcus mutans* is a facultatively anaerobic, Gram-positive bacterium and a group of lactic acid bacteria commonly found in the human oral cavity and is a significant contributor to tooth decay. Streptococci represent 20% of the oral bacteria and, along with sucrose, essentially determine the development of biofilms.14-16 Even though *Streptococcus mutans*

could be antagonized by the leading oral colonists, once they become dominant in mouth biofilms, tooth decay can develop and thrive. While *S. mutans* grow in biofilm cells maintain a balance of metabolism involving the production and detoxification reactions. Biofilm is the sum of microorganisms and can actually generate various toxic compounds that interfere with the growth of other competing bacteria [Hamada & Slade 1980].



# Chapter 3

## Materials and Methods

This chapter provides an overview of the experimental procedures that were followed to fulfill the aims and objectives of this study. It represents the motive for the choice of the green biosynthesis method and the techniques used in the study and the experimental approach followed in pursuit of the objectives of this study. Several activities were covered in this chapter, including: 1) selection and screening of different plants extracts; 2) preparation of the aqueous extracts; 3) synthesis of nanoparticles; and 4) characterization of the nanoparticles *via* different characterization techniques; 5) antimicrobial activity test.

### 3.1 Materials and Instruments

Gold salt (sodium tetrachloroaurate(III) dihydrate) and silver nitrate were purchased from Sigma-Aldrich (Cape Town, South Africa), 96-well microtitre plates were obtained from Greiner Bio-One GmbH (Frickenhausen, Germany). Alamar blue dye was obtained from Invitrogen Corporation (San Diego, CA, USA). *Streptococcus mutans* ATCC ® 25175<sup>TM</sup> was obtained from Quantum Biotech. Neomycin antibiotic was purchased from Sigma-Aldrich (Cape Town, South Africa). Brain heart infusion and nutrient broth were purchased from Quantum Biotech (Cape Town, South Africa). Centrifugation for the extracts was done using Allegra® X-12R (Beckman Coulter, Cape Town, South Africa). The extracts were freeze-dried using FreeZone 2.5 L (Labconco, Kansas City, MO, USA).

UV-Vis spectra were recorded using POLARstar Omega microplate reader (BMG Labtech, Cape Town, South Africa). The particle size, size distribution and zeta potential measurements of the freshly synthesized NPs in solution were analyzed using Zeta Sizer (Malvern Instruments Ltd., Malvern, UK). The NPs were centrifuged using Centrifuge 5417R (Eppendorf AG, Hamburg, Germany). TEM analysis was done using FEI Tecnai G2 20 field-emission gun (FEG) High Resolution Electron Microscope. The crystallographic properties were recorded by using X-ray Diffraction (XRD) Model smart lab (Cuka:  $\alpha=1.5406 \text{ \AA}$ ), operating at a current of 200 mA and a voltage of 45 kV in Bragg-Brentano geometry.

### **3.2 Plant collection and extract preparation**

The plant species under this study were collected from North African region after getting the required collection permits. Plant samples are represented in Table 3.1. The aerial parts of each plant were collected randomly from Northern area of Libya “called the Green Mountain” during April and May 2016. Figure (2.1) is representing all collected plant samples. After collection, the fresh samples were cleaned and dried in shade for two weeks, then grinded. Powder materials were packed and stored at 4 °C until use. Plant materials were extracted “separately” by adding a fixed amount of powder to boiled distilled water (50 mL distilled water/5 g plant) with shaking for a period of (30 minutes – 1.0 h). The supernatants were centrifuged at 3750 rpm for one hour to remove the solid materials using an Allegra® X-12R centrifuge (Beckman Coulter, Cape Town, South Africa). The supernatant for each extract was then filtered through 0.45 µm filters, and freeze dried using free zone 2.5L freeze dryer (Labconco, USA). A stock solution of 10 mg/mL was freshly prepared for each extract before the screening step.

**Table 3.1:** List of the collected plant species from the Green Mountain area “Libya”

No	Plant name	Family	Herbarim No.
1	<i>Pistacia atlantica</i>	ANACARDIACEAE	S17
2	<i>Anethum graveolens</i>	APIACEAE	S20
3	<i>Pituranthos tortuosus</i>		S16
4	<i>Artemisia absinthium</i>	ASTERACEAE	S6
5	<i>Artemisia herba-alba</i>		S10
6	<i>Chamomilla pubescens</i>		S1
7	<i>Helichrysum stoechas</i>		S14
8	<i>Juniperus phoenicea</i>	CUPRESSACEAE	S2
9	<i>Retama raetam</i>	FABACEAE	S18
10	<i>Ajuga iva</i>	LAMIACEAE	S5
11	<i>Marrubium vulgare</i>	LAMIACEAE	S7
12	<i>Rosmarinus officinalis</i>		S15
13	<i>Salvia officinalis</i>		S19
14	<i>Thymus capitatus</i>		S13
15	<i>Teucrium polium</i>		S8
16	<i>Globularia alypum</i>	PLANTAGINACEAE	S3
17	<i>Cymbopogon schoenanthus</i>	POACEAE	S12
18	<i>Peganum harmala</i>	NITRARIACEAE	S11
19	<i>Ziziphus lotus</i>	RHAMNACEAE	S4
20	<i>Ruta graveolens</i>	RUTACEAE	S9



*Pistacia atlantica*



*Anethum graveolens*



*Pituranthos tortuosus*



*Artemisia absinthium*



*Artemisia herba-alba*



*Chamomilla pubescens*



*Helichrysum stoechas*



*Juniperus phoenicea*



*Retama raetam*



*Ajuga iva*



*Marrubium vulgare*



*Rosmarinus officinalis*

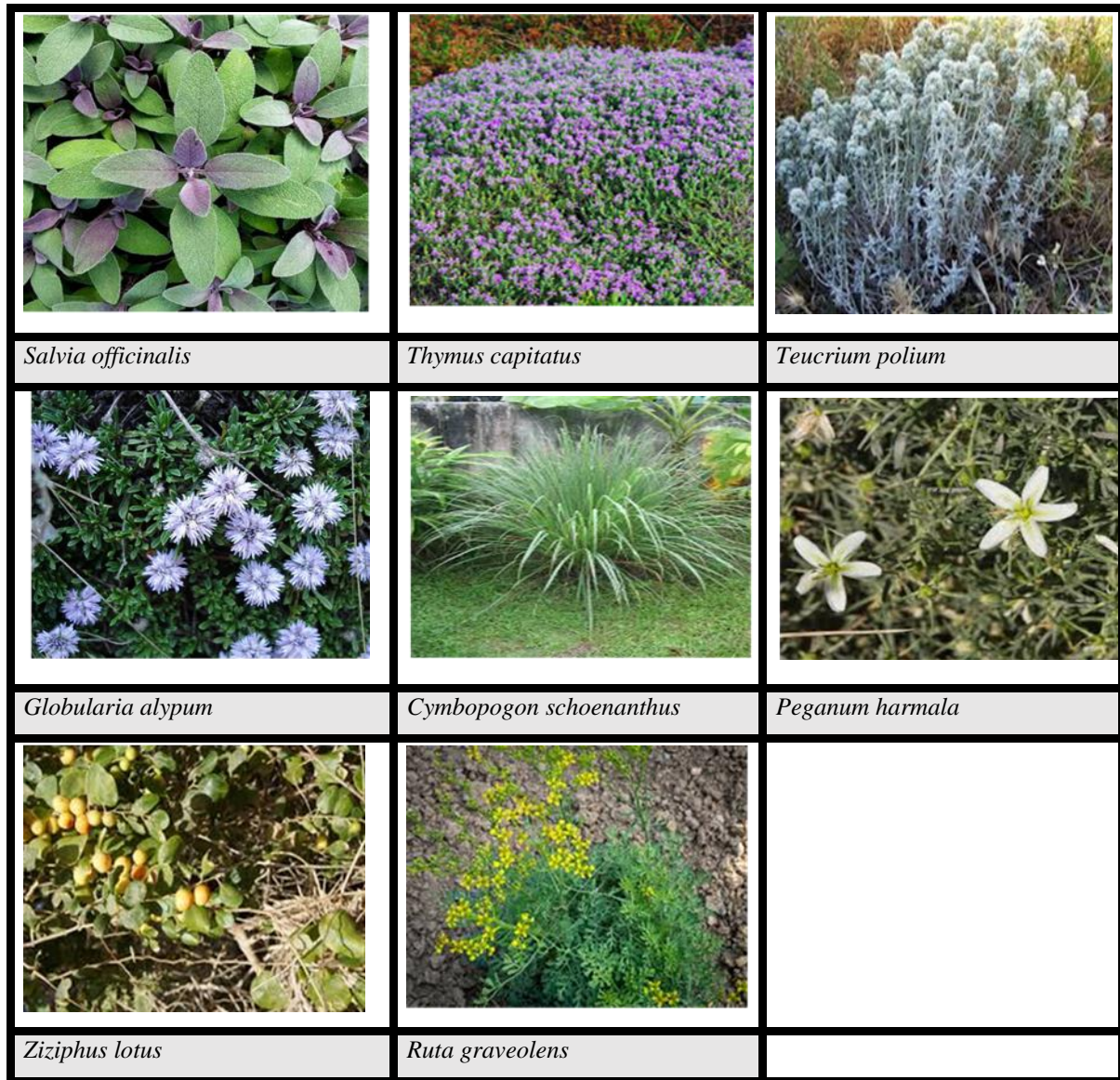


**Figure 3.1:** Aerial parts of the selected plant species under study.

### **3.3 Biosynthesis of the gold and silver nanoparticles (Au and Ag NPs)**

Gold and silver salts were added separately at a concentration of 1 mM and 3 mM, respectively in 96-well plates to test the reducing ability of the selected plant extracts. Also, different concentrations of plant extracts (from 10.0 to 0.0195 mg/300  $\mu$ L) were used. These different concentrations of extracts were obtained by serial dilution. 250  $\mu$ L of gold or silver salt were added to 50  $\mu$ L of the increased concentrations of plant extracts by (ratio 5:1) in every 96-well plate separately.

Interactive activity was observed at two different temperatures by incubating the samples at 96-well plates, at 25 °C and 70 °C for one hour, while stirring at 40 rpm. It was measured and confirmed by recording the UV-Vis spectrum from range 300 nm to 800 nm in the above-mentioned conditions and adding 200  $\mu$ L of nanoparticles synthesized to 100  $\mu$ L of sterile dH<sub>2</sub>O by ratio 2:1 in each hole using a POLAR star Omega microtitre plate reader (BMG Labtech, Germany). Concentrations were selected from the extracts that gave the best peak in the initial test. By raising the level of tests for the three selected concentrations to the final volume of 1.5 ml or 3 ml in a sterile dH<sub>2</sub>O warehouse in Eppendorf tubes or vials. Concentration ratios were adjusted to be appropriate for scale-up volumes to maintain a ratio of reagents. After all the samples were incubated under the same conditions above, the nanoparticle solution was centrifuged twice at 10000 rpm, for 10 minutes at 25 °C using sterile dH<sub>2</sub>O. The centrifuge 5417R (Eppendorf AG, Germany) was used to purify and concentrate the nanoparticles. The nanoparticles were re-suspended in sterile dH<sub>2</sub>O to 10 mg/mL stock solution.

### **3.4 Characterization techniques**

#### **3.4.1 UV visible spectroscopy**

It is one of the popular characterization techniques to determine particle formation and its optical properties. It refers to absorption spectroscopy or reflectance spectroscopy in the ultraviolet-visible spectral region UV-Vis absorbance spectroscopy was carried out to monitor the formation of nanoparticles (with a SPECTROstar Nano, BMG labtech UV-Vis spectrophotometer). The UV-Vis absorption spectra were recorded immediately after the preparation.

### **3.4.2 Dynamic light scattering (DLS) Analysis**

DLS was used to measure the hydrodynamic size and zeta potential at 25 °C. 1.0 mL of the synthesized NPs was placed in the cuvette. The measurement was done three times and the average was calculated for the hydrodynamic size and the charge. These measurements were performed on all samples and selected concentrations.

### **3.4.3 High resolution transmission electron microscopy (HR-TEM) and energy dispersive X-ray spectroscopy (EDS) analysis**

Samples were prepared for the study of the surface morphology of the biosynthesized NPs by placing one drop of each sample on the surface of the carbon-coated copper mesh. The samples were dried under the light of the xenon lamp for 10 minutes. Elemental analysis of the NPs was done by recording the EDS- spectra of the samples. The TEM analysis of the sample coated grids was done by monitoring TEM images. The size of the nanoparticles was determined with ImageJ software.

### **3.4.4 X- ray diffractometer (XRD)**

The structure and crystallinity of lyophilized powdered samples of nanoparticles (Ag NPs and Au NPs ) were analysed using XRD. The XRD patterns were acquired from Model smart lab (Cuka;  $\alpha_1=1.5406 \text{ \AA}$ ) refractometer operating at a current of 200 mA and a voltage of 45 kV in Bragg-Brentano geometry, scan speed 2,000 degree/min. It is an essential technique for phase identification and crystal structure refinement. The XRD spectra were recorded in a specific range using an X-ray source of Cu K $\alpha$  ( $\lambda=0.154 \text{ nm}$ ) monochromatic radiation.

### **3.5 Stability analysis**

The stability of the synthesized NPs in different biological media was determined by incubating the NPs in the media for a period of 24 h. First, the NPs were centrifuged at 10,000 rpm for 5 min. The pellets were washed three times with distilled water to remove phytochemicals that are not capping the gold nanoparticles. The NPs were re-suspended in 1 mL autoclaved distilled water and 50  $\mu\text{L}$  was added to 150  $\mu\text{L}$  of selected biological media for tests by (rate 3:1). The mixture was incubated at 37 °C for 24 hours in a 96-well microtitre

plate. The stability of the NPs was evaluated by measuring the changes in UV-Vis spectra after 0, 2, 4, 6, 12 and 24 h using a POLARstar Omega microtitre plate reader (BMG Labtech, Germany).

### 3.6 Antibacterial evaluation

Three plant extracts “*P. atlantica*, *J. phoenicea*, and *R. officinalis*” with their corresponding NPs (Ag and Au NPs) were selected further for antibacterial evaluation against *S. mutans*. The Alamar blue assay was used to evaluate the inhibition of bacterial growth against *S. mutans* ATCC ® 25175, by both the NPs and the plant extracts. The bacterial strains activated in brain heart infusion medium at room temperature and incubated for 24 hours at 37 °C while shaking overnight. The bacteria were transferred into nutrient broth media after centrifugation. The density was adjusted at 0.5 OD at 450 nm (McFarland standard) using a Polystar Omega microplate reader to maintain the final number of  $5 \times 10^6$  CFF. Bacteria were incubated overnight for 24 hours at 37 °C. Activity against bacteria was observed by the level of turbidity change after incubation for 24 hours.

To determine the MIC values of the tested samples, 150 µl of bacterial broth was mixed in a 96 microtitre plate with 50 µl of NPs and plant extracts (concentrations ranged from 50 to 0.039 µg/mL). Neomycin antibiotic was used as a positive control. Positive controls were also prepared by mixing 150 µL of bacterial culture with 50 µL of nutrient broth (concentrations ranged from 50 to 0.039 µg/mL). The plates were incubated at 37 °C for 24 hours, after which 10.0 µL of Alamar blue dye was added to each well. Additional plates were incubated for 2 hours. Absorbance was then recorded at 570 nm. To assess whether the NPs and plant extracts interfere with the Alamar blue probe, a control sample was also prepared by mixing 50 µL of NPs and plant extracts (for each concentrations) with 150 µL of nutrient broth.



# Chapter 4

## Results and Discussion

Twenty plant species were randomly collected from the Green Mountain area in the northern part of Libya. The plants were documented and extracted using water. The aqueous extracts were tested for their ability to form a stable metal NPs with Au and Ag.

The synthesis of the NPs particles went through two phases:

- 1- Screening of the 20 extracts according to the previous designed protocol [El-Bagory et al., 2016] and determining the most appropriate extract(s) to synthesis the metal NPs. The quality of the NPs produced was judged through the investigation of different characterization techniques such as UV, DLS, TEM, EDS, and XRD. The stability study was performed as well.
- 2- The selected extract(s), was further evaluated for more informations in terms of kinetics and antibacterial activity.

In this chapter, the results obtained from these techniques will be discussed.

Some of the selected plant materials have been used extensively in Libyan traditional medicine, for example *P. atlantica*, *A. absinthium*, *A. herba-alba*, *J. phoenicea* and *R. officinalis* are well-known and widely distributed among the traditional healers and incorporated into many herbal formulations for treatment of different human diseases. The details of each of these plants were given in section 2.5 of the literature review.

### 4.1 Determination of the optimum concentration

As previously reported twenty plants were collected, extracted and been used for synthesizing gold and silver nanoparticles. Figure 4.1 reveals the efficiency of all selected plants for synthesizing gold NPs at 70 °C. Some extracts showed decreased efficiency at lower temperature (25 °C). The initial results confirmed the importance of temperature in the synthesis process of NPs. Changes in the color is considered as the first indication for the formation of gold NPs. The results show the color changing from yellow to red based on the temperature and concentration.

On the other hand, Figure 4.2 represents the effect of temperature and concentration of the twenty plants extracts on the formation of silver NPs. The results show that only fifteen

plant extracts were able to produce silver nanoparticles at 70 °C. The variation in reducing power on the 20 species is expected because of the different chemical constituents exist in each species [El-Bagory et al., 2016]. Additionally, the results confirmed the effect of temperature and incubation time on the synthesis process. The initial indication for the formation of silver NPs is the change in the color to yellow and dark brown. The color density of nanoparticles increased with increasing reaction time. The phenomenon that makes this observation possible is called surface plasmon resonance (SPR), which is unique to metallic nanoparticles and gives a characteristic wavelength of certain metallic particles that depends on the shape and size of nanoparticles.

The results in Figures 4.1 and 4.2 reveal that the optimum concentration (OC) is variable based on the plant species. Generally, it was observed that the OC decreased with the increase in temperature as can be seen in Tables 4.1 and 4.2. This is directly related to the activation energy acquired at higher temperature which facilitates and speeds up the chemical reaction. Similar results were observed in a study of local plant extracts from South Africa [El-Bagory et al. 2016].



**Figure 4.1:** The screening of the selected plant extracts for the biosynthesis gold NPs at 25 °C and 70 °C

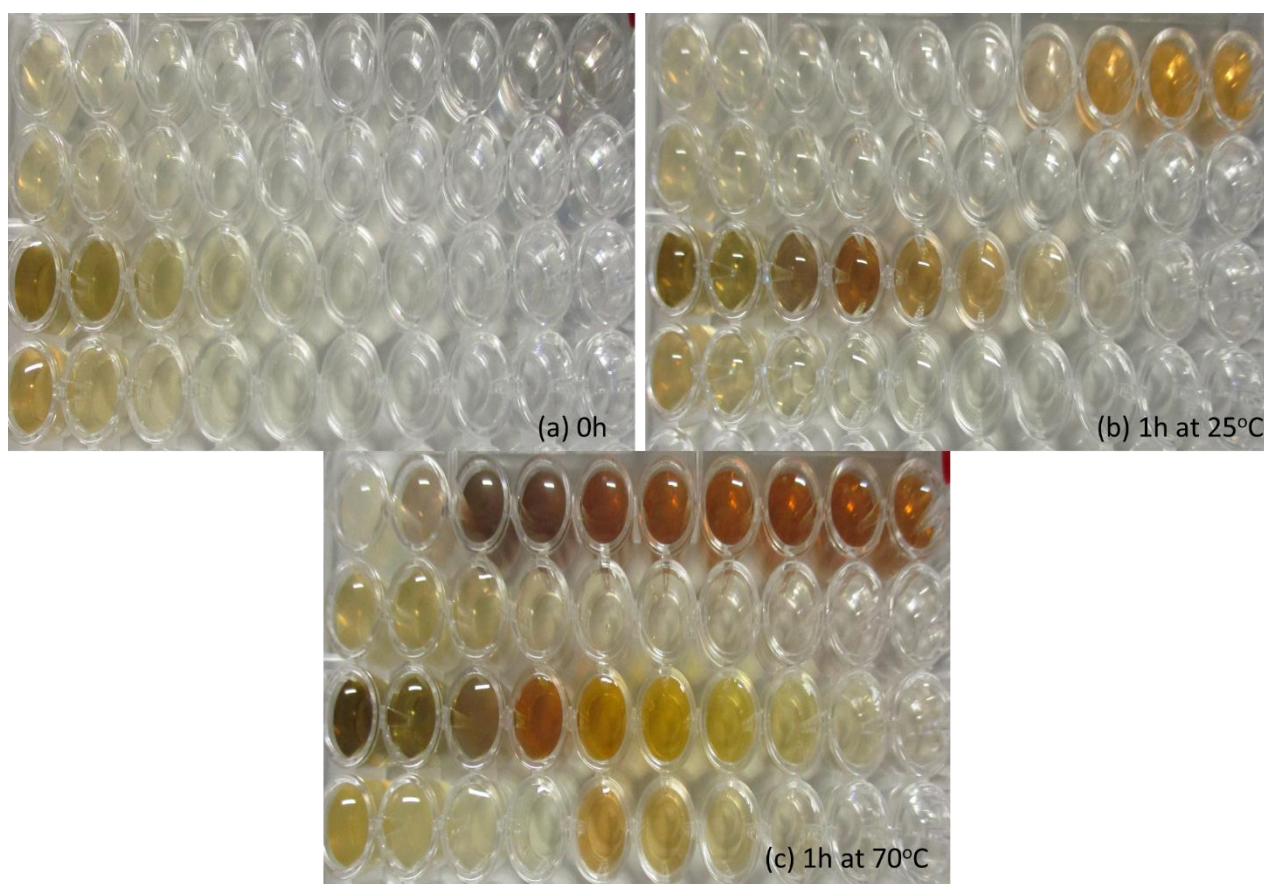


**Figure 4.2:** The screening of the selected plant extracts for the biosynthesis silver NPs at 25 °C and 70 °C

## 4.2 Characterisation of the biosynthesized nanoparticles

### 4.2.1 Uv–vis spectrophotometric analysis

When an object is subjected to a light beam, it absorbs certain photons while others get transmitted, scattered or reflected. Therefore, measuring the interaction of light with an object can predict the presence and size of that object. The maximum absorbance ( $\lambda_{\max}$ ) indicates the wavelength at which the nanoparticles absorb. The shift towards longer wavelengths represents an increase in average particle size and *vice versa*.

Preliminary characterization of the silver and gold NPs was performed to investigate the optical properties of the synthesised NPs. Controlling the size, shape, and stability of nanoparticles are important factors for effective industrial applications [Mishra et al. 2011]. Time-dependent formation of silver and gold NPs was observed using uv–vis.

spectrophotometer. The very first indication for success of nanoparticle synthesis is the change in colour. The colour changes were due to the excitation of surface plasmon vibrations, which is a characteristic feature of synthesized nanoparticles [Song et al. 2009]. For the Au NPs the colour change from red/red wine to sapphire red and for Ag NPs from yellow/yellow-brown to dark brown (Figures 4.1 and 4.2).

Figures 4.3 and 4.4 depict the uv-vis spectra of a typical gold and silver NPs solution at different temperatures. It was observed that the maximum absorptions of gold NPs represented in Table 4.1 where it occurs between 500 and 600 nm. On the other hand, Table 4.2 shows that the absorption of the biosynthesized silver NPs occurs between 400 and 500 nm due to SPR .

Five plant extracts, *A. graveolens*, *A. iva*, *M. vulgare*, *G. alypum*, and *P. harmala* did not change colour when they tested with gold salt at 25 °C (Table 4.1). While for silver NPs; *A. graveolens*, *P. tortuosus*, *R. raetam*, *A. iva*, *P. harmala*, *C. pubescens*, *M. vulgare*, *S. officinalis*, *T. polium*, *C. schoenanthus*, and *R. graveolens* showed no change in colour at the same temperature (25 °C) (Table 4.2). These results directly related the chemical constituents of each of the tested plant extracts, which is the main factor when compared with other potent extracts.

The shape of surface plasmon peaks is also affected; at higher temperature (70 °C) a sharp peak was observed compared to the one at room temperature (25 °C). This could be attributed to an increase in the efficiency of the reaction. This observation may refer to the generation of smaller, more consistent particles that appear to be more favourable because the nanoparticles formed are better defined. At 70 °C, the reaction can also result in higher production of nanoparticles where higher optical density has been observed that can give an indication of the concentration of nanoparticles produced in specific reaction conditions. At low temperatures, the chemical reaction is much slower, leading to lower productivity and giving chances for size increase. This also, may be attributed to the rate of the reaction of the chemical constituents in each plant extract. This was observed by Dzimitrowicz et al. 2019 who demonstrated through the results of ATR-FTIR analysis of environment-friendly Au NPs which revealed multiple compounds involved in Au NPs synthesis of different extracts. There are many factors that contribute to differences in size and other physical-chemical properties including changes in incubation time, temperature, and the chemical constituents of the plant extract [Dzimitrowicz et al., 2019]. The absorption at the longer wavelength is attributed to SPR stimulation and indicates significant variation in the shape of nanoparticles and mainly

the formation of spherical NPs. The maximum absorption data was recorded from all tested plants.

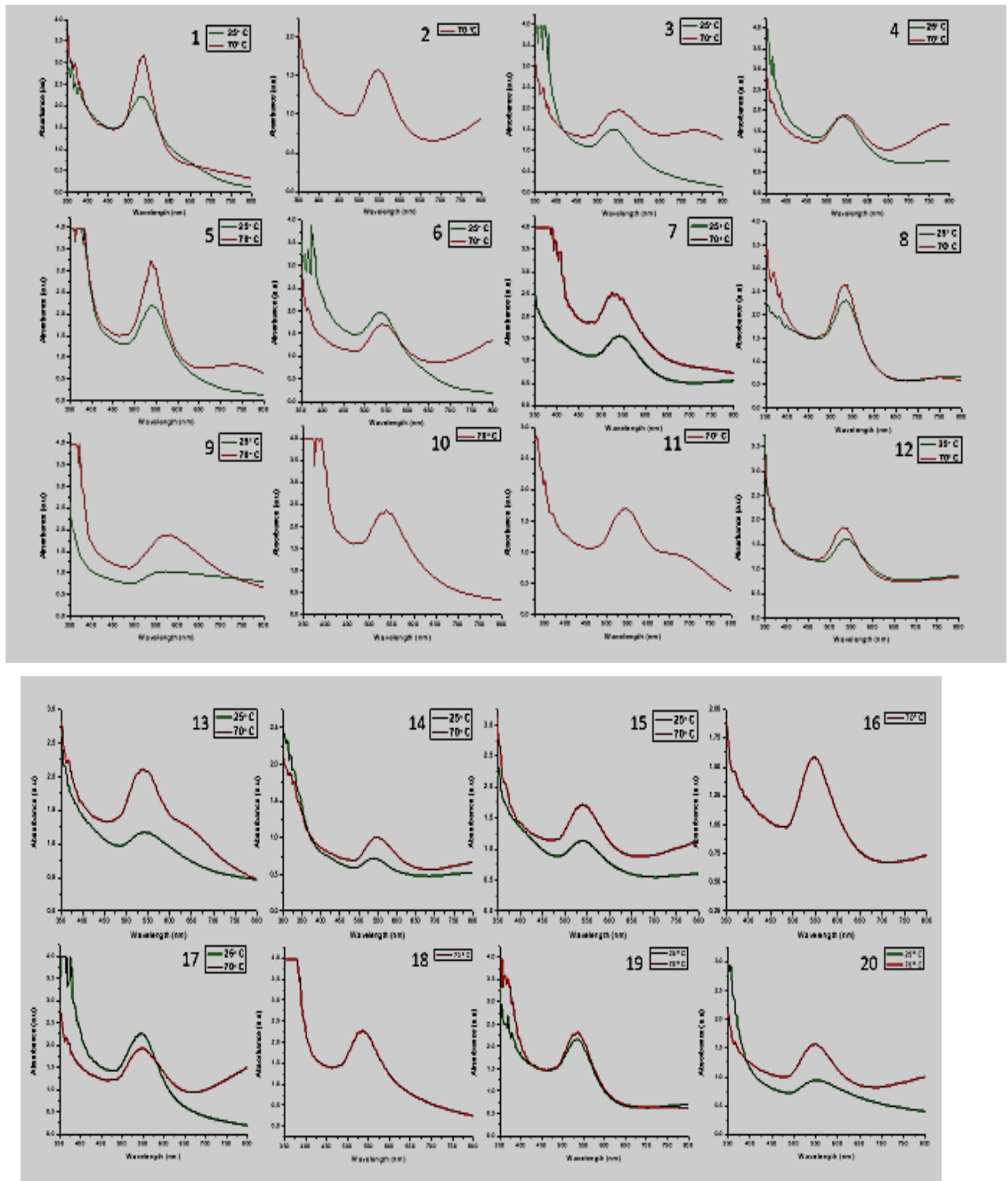


Figure 4.3: Comparison of the UV spectra of Au NPs produced at 25 (green curves) and 70 °C (red curves)

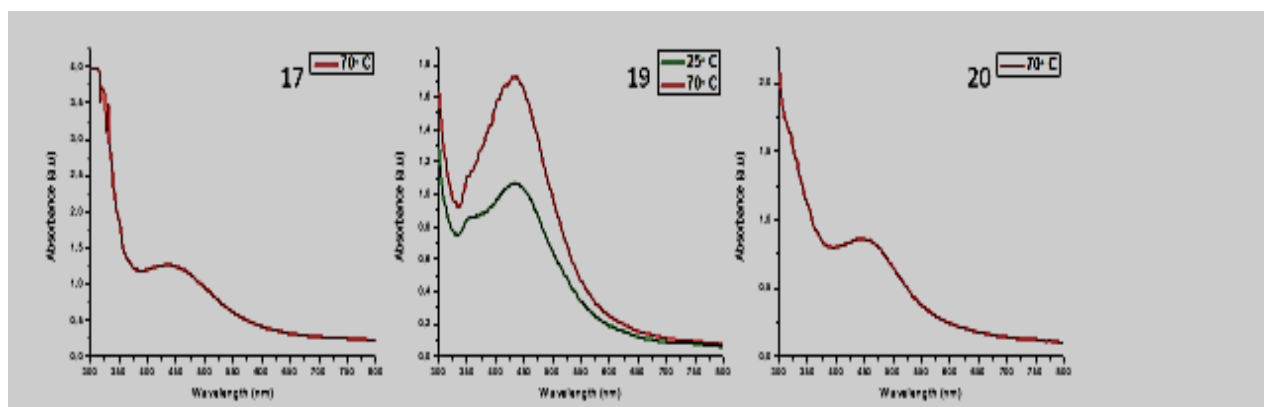
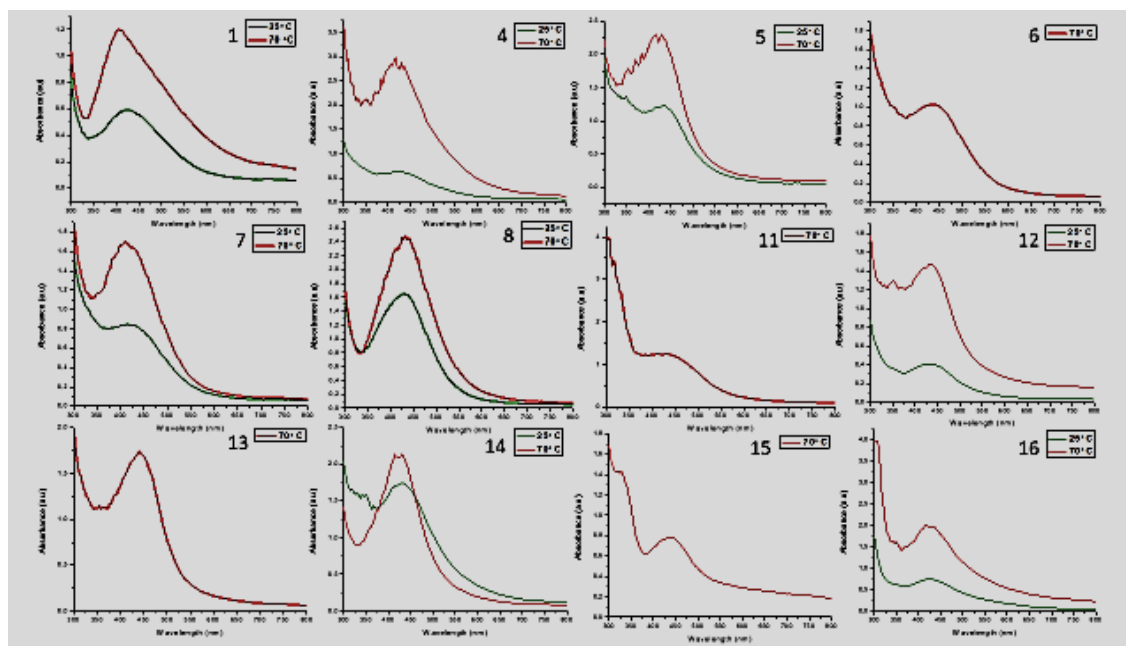


Figure 4.4; Comparison of the UV spectra of Ag NPs produced at 25 (green curves) and 70 °C (red curves)

#### 4.2.2 Dynamic light scattering analysis

Dynamic light scattering (DLS) was used to determine parameters such as size (average diameter), polydispersity index (PDI) and zeta potential (ZP) of the biosynthesized nanoparticles. Tables 4.1 and 4.2 represent the average results of the synthesized nanoparticles from the twenty Libyan plant species. The size of the nanoparticle remains the most important parameter as the chemical and physical characteristics of the nanoparticle associated with their function are dependent on it. One of the important features of NPs is its surface- to volume ratio which is inversely proportional to the diameter of the nanoparticle. The smaller the nanoparticle, the larger its surface area and therefore more binding sites for various applications such as drug and gene delivery. The effects caused by the different reaction conditions which were studied under controlled conditions were assessed by DLS to observe the influence of these parameters on the particles' size. The changes were observed to be unique to each plant extract from which the NPs have been derived [Lee et al., 2014]. DLS results showed the average diameter of the synthesized Au NPs within the range of 27-157 nm at room temperature and 12 - 119 nm at 70 °C. The wide range in size may be attributed to the efficiency of each plant to work as a reducing agent as well as an effective capping agent.

The results reveal that, *P. atlantica* and *S. officinalis* were the most effective extracts out of the 20 plants tested in this study in terms of facilitating the production of Au NPs with an average size of 27 nm at 25 °C and 12 nm at 70 °C, respectively. On the other hand, the synthesized Ag NPs from these twenty plants had an average diameter within a range of 20 - 154 nm at room temperature and 37-161 nm at 70 °C. *A. herba-alba* and *G alypum* were observed to be the best plant extract out of the 20 plants tested in this study in terms of facilitating the production of Ag NPs with an average size of 20 nm at 25 °C and 37 nm at 70 °C, respectively. The size of biosynthesized Au NPs is greatly affected by the type of compounds in the extracts used for the synthesis process. In this study, smaller nanoparticles were also observed at a higher temperature than at low temperature, also the decrease of the extract concentration produce smaller nanoparticles [Cele et al., 2009].

The PDI shows the measure of molecular mass distribution of the synthesized nanoparticles. The results showed that some plants had higher PDI at room temperature while others had insignificant differences at the different temperature conditions which may attribute to the heterogeneity of the chemical components of the plants. *C. schoenanthus* and *S. officinalis* showed efficiency in the synthesis process of Au NPs at 70 °C with an average

diameter of 33 and 12 nm, respectively. These results were in agreement with the UV-vis spectroscopy analysis where it shows SPR peaks at 546 and 526 nm, respectively.

The variations observed in the average diameter of the Au NPs synthesized from the two extracts could be due to the contribution of the organic layer which is dependent on plant constituents [Yu 2007]. The behaviour of the phytochemicals at different temperatures could contribute to their effectiveness in reducing the gold salt to nanoparticles. Hence, the complexity of the phytochemicals presents in the plant extracts and their unique characteristics seems to be the main factor that could be contributing to the unpredictable results of the reaction products in this study. It is worth stating that the nanoparticles were observed to be fairly stable regardless even though the zeta potential is being below the acceptable range of stability observation by this method. All the plants gave rise to Au NPs with a negative zeta potential which corresponds to a negative surface charge of the nanoparticles. This negative surface charge leads to greater stability of the nanoparticles through columbic repulsion forces that are induced by this surface charge leading to decreased aggregation of the nanoparticles [Lukman et al. 2011]. Hence, zeta potential measurements were an effective parameter in the final selection of the best plant extract in the biosynthesis process. The ZP results show more stability of the resultant Au NPs at the high temperature of the synthesis process.

**Table 4.1.** The optimum concentration (OC), particle diameter (PD), polydispersity index (Pdi),  $\lambda_{\max}$  and average zeta potential values (ZP) of the Au NPs synthesised from the tested plant extracts at 25 °C and 70 °C.

No	Plant Name	25 °C					70 °C				
		OC (mg/mL)	Pdi	PD (nm)	$\lambda_{\max}$ (nm)	ZP (mV)	OC (mg/mL)	Pdi	PD (nm)	$\lambda_{\max}$ (nm)	ZP (mV)
1	<i>P. atlantica</i>	0.31	0.711	27	526	-13	0.15	0.666	24	538	-20
2	<i>A. graveolens</i>	#	#	#	#	#	0.62	0.476	48	546	-16
3	<i>P. tortuosus</i>	5.00	0.638	30	538	-16	0.62	0.645	28	538	-15
4	<i>A. absinthium</i>	2.50	0.516	42	536	-15	0.62	0.628	29	546	-15
5	<i>A. herba-alba</i>	5.00	0.447	50	540	-19	2.50	0.442	55	538	-20
6	<i>C. pubescens</i>	5.00	0.653	154	536	-17	0.62	0.487	56	538	-11
7	<i>H. stoechas</i>	1.25	0.440	55	542	-15	2.50	0.845	36	524	-17
8	<i>J. phoenicea</i>	0.62	0.436	46	536	-13	0.62	0.513	40	536	-16
9	<i>R. raetam</i>	2.50	0.261	469	572	-13	5.00	0.222	794	584	-13
10	<i>A. iva</i>	#	#	#	#	#	2.50	1.000	16	538	-18
11	<i>M. vulgare</i>	#	#	#	#	#	0.62	0.604	33	550	-14
12	<i>R. officinalis</i>	0.62	0.515	67	540	-17	0.31	0.455	55	532	-20
13	<i>S. officinalis</i>	2.50	0.582	39	542	-18	5	0.944	12	526	-17
14	<i>T. capitatus</i>	0.62	0.490	116	542	-16	0.31	0.450	78	550	-20
15	<i>T. polium</i>	1.25	0.482	109	538	-14	0.62	0.520	43	538	-13
16	<i>G. alypum</i>	#	#	#	#	#	0.31	0.451	65	548	-19
17	<i>C.schoenanthus</i>	5.00	0.609	34	546	-11	0.62	0.621	33	546	-16
18	<i>P. harmala</i>	#	#	#	#	#	5.00	0.351	119	536	-24
19	<i>Z. lotus</i>	1.25	0.554	36	534	-13	1.25	0.639	26	538	-16
20	<i>R. graveolens</i>	2.50	0.436	117	542	-13	0.625	0.317	77	552	-14

# No nanoparticles were formed at this condition.

**Table 4.2.** The optimum concentration (OC), particle diameter (PD), polydispersity index (Pdi),  $\lambda_{\max}$  and average zeta potential values (ZP) of the Ag NPs synthesized from the tested plants at 25 °C and 70 °C.

No.	Plant Name	25 °C					70 °C				
		OC (mg/mL)	Pdi	PD (nm)	$\lambda_{\max}$ (nm)	ZP (mV)	OC (mg/mL)	Pdi	PD (nm)	$\lambda_{\max}$ (nm)	ZP (mV)
1	<i>P. atlantica</i>	0.02	0.380	109	420	-33	0.02	0.639	119	414	-32
2	<i>A. graveolens</i>	#	#	#	#	#	#	#	#	#	#
3	<i>P. tortuosus</i>	#	#	#	#	#	#	#	#	#	#
4	<i>A. absinthium</i>	0.31	0.492	50	418	-26	0.62	0.682	40	418	-23
5	<i>A. herba-alba</i>	2.50	0.617	20	414	-24	0.62	0.343	54	432	-26
6	<i>C. pubescens</i>	#	#	#	#	#	0.31	0.472	77	432	-26
7	<i>H. stoechas</i>	0.31	0.418	154	416	-18	0.31	0.525	112	412	-25
8	<i>J. phoenicea</i>	2.50	0.659	40	428	-16	1.25	0.369	83	430	-18
9	<i>R. raetam</i>	#	#	#	#	#	#	#	#	#	#
10	<i>A. iva</i>	#	#	#	#	#	#	#	#	#	#
11	<i>M. vulgare</i>	#	#	#	#	#	1.25	0.604	136	414	-17
12	<i>R. officinalis</i>	0.15	0.589	39	436	-35	0.15	0.588	55	436	-22
13	<i>S. officinalis</i>	#	#	#	#	#	1.25	0.715	101	438	-27
14	<i>T. capitatus</i>	0.62	0.640	31	420	-20	0.31	0.504	51	428	-21
15	<i>T. polium</i>	#	#	#	#	#	0.31	0.689	161	438	-19
16	<i>G. alypum</i>	0.15	0.601	52	430	-30	0.31	0.537	37	416	-17
17	<i>C.schoenanthus</i>	#	#	#	#	#	1.25	0.527	44	434	-19
18	<i>P. harmala</i>	#	#	#	#	#	#	#	#	#	#
19	<i>Z. lotus</i>	0.62	1.000	26	432	-21	2.50	0.600	63	432	-20
20	<i>R. graveolens</i>	#	#	#	#	#	0.62	0.493	234	444	-18

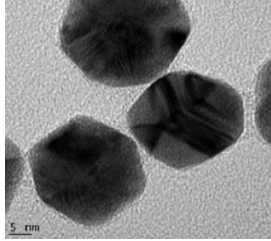
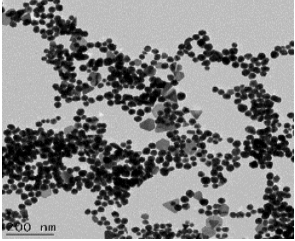
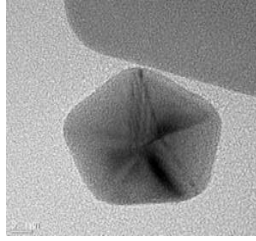
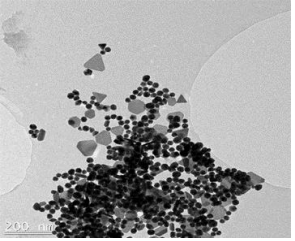
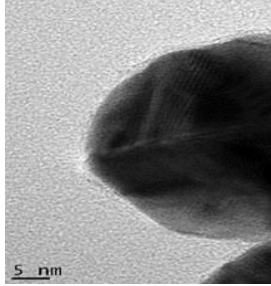
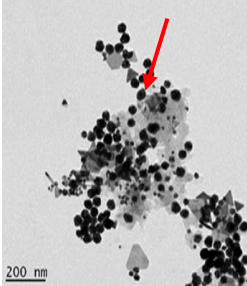
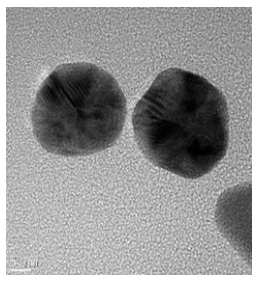
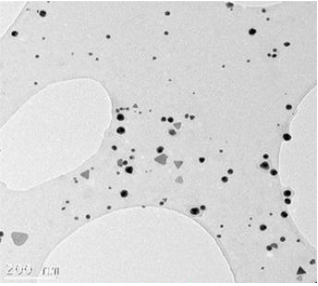
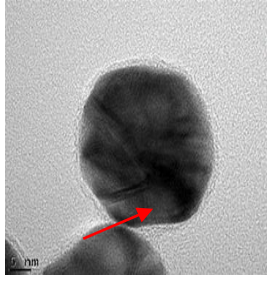
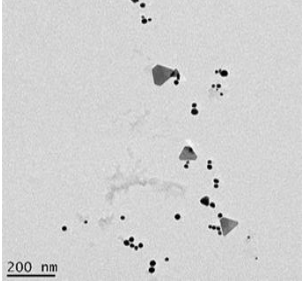
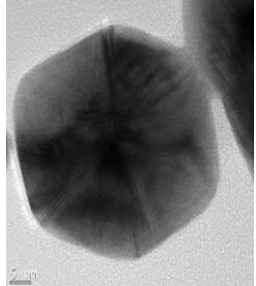
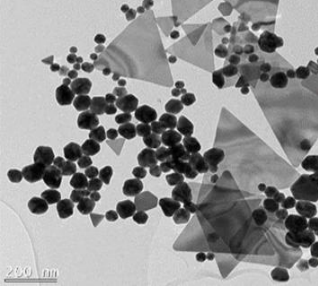
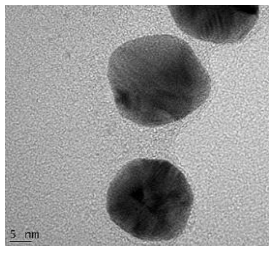
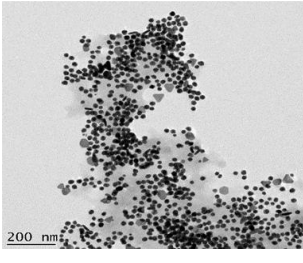
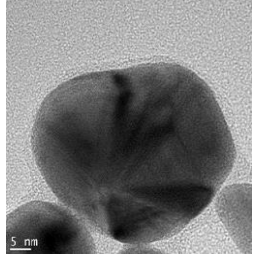
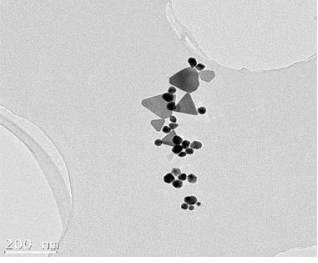
# No nanoparticles were formed at this condition.

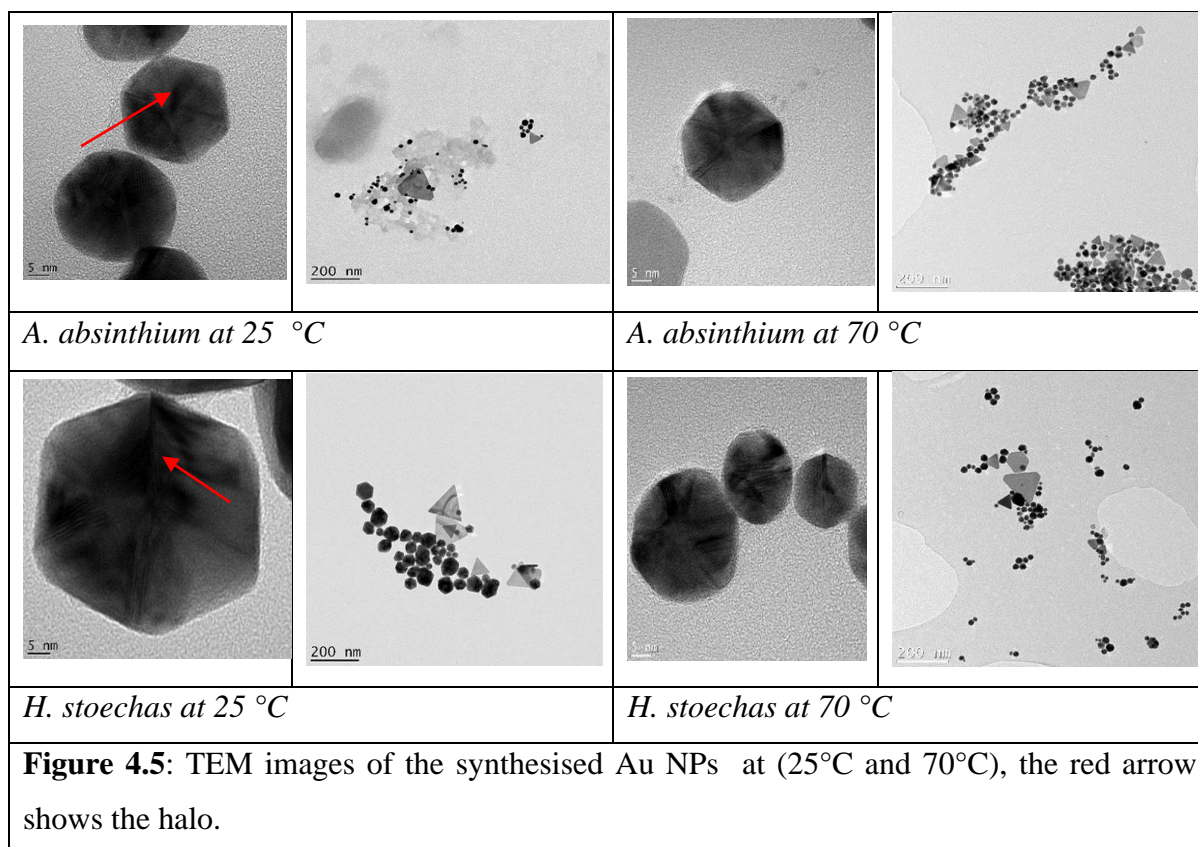
### 4.2.3 High resolution-Transmission Electron Microscopy (HR-TEM ) analysis

The TEM images of the biosynthesized selected samples are shown in Figures (4.5 and 4.6). The results show variable geometrical shapes and sizes based on the tested plant extract. The EDS results have also been included in this study. The nanoparticles synthesized from the different extracts revealed various shapes and relative sizes as observed from the TEM images (Figure 4.5).

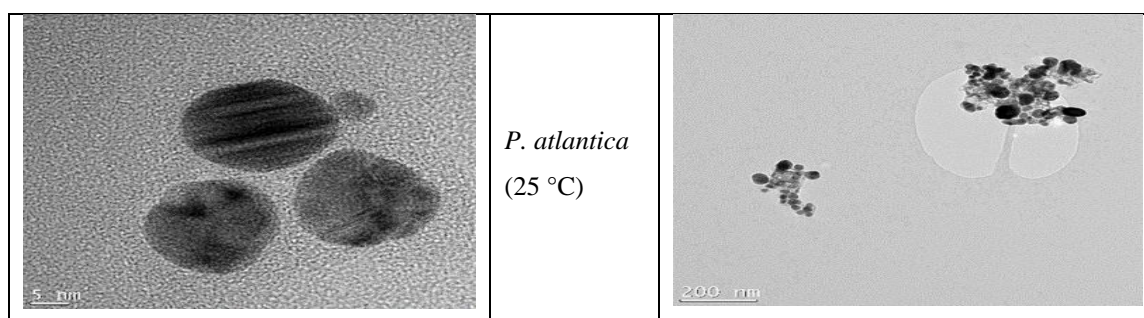
Shapes such as spheres, pentagons, hexagons, and triangles were observed among the biosynthesized Au NPs. Gold spheres and pentagons being the most dominant. Overall, larger particles from ~ 150 nm in size were mostly triangular, truncated triangular, and hexagonal in shape. On the other hand, smaller nanoparticles were mostly, spherical, pentagonal and hexagonal. This mixture of geometrical shapes is a common feature of Au NPs as reported before [Chen et al. 2010; Foss et al. 1994], and is attributed to the different phytochemicals reducing agents in the plants extracts. The results also reveal that temperature in synthesis reaction plays a role in the shape, and size of the nanoparticles. For example, it is observed that at 25 °C the nanoparticles are more uniform in shape and size compared to those synthesized at 70 °C. The dominant shapes in both conditions were hexagonal and spherical, although triangular and pentagonal shapes were also observed. The nanoparticles were observed to be smaller at 70 °C but more, heterogeneous at 70 °C compared to 25 °C.

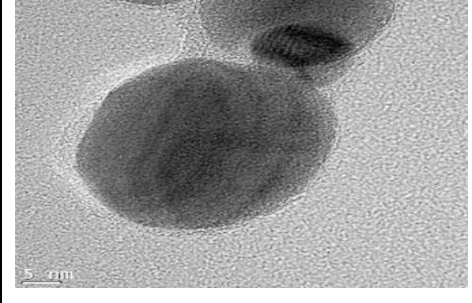
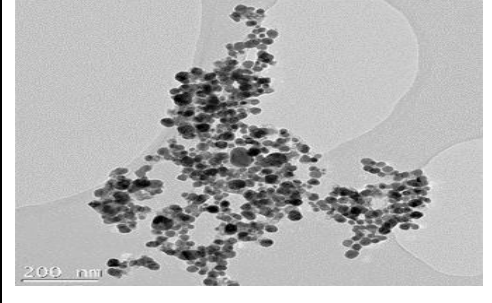
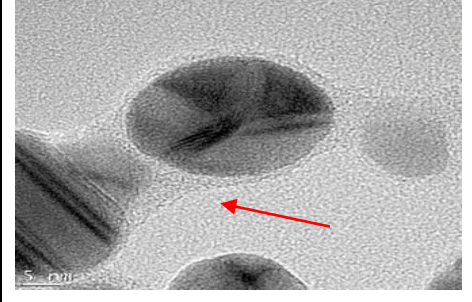
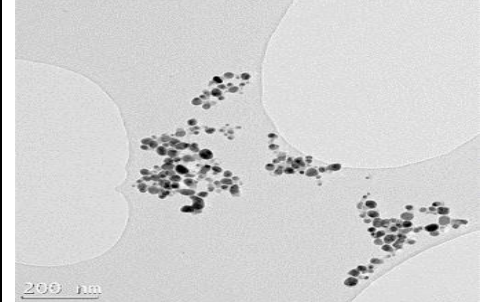
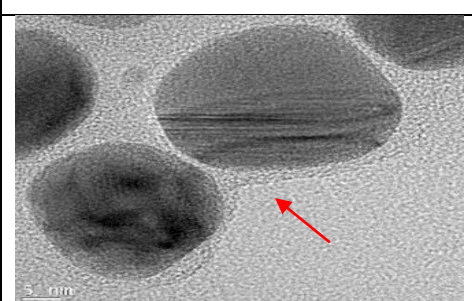
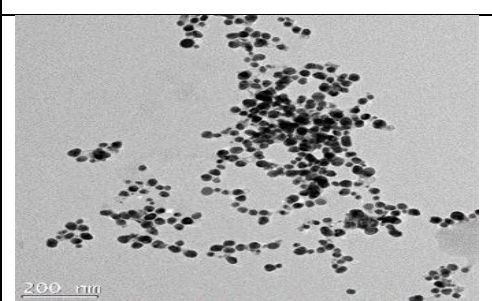
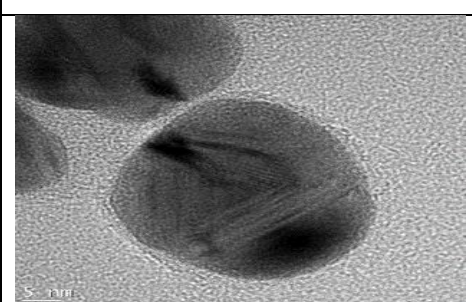
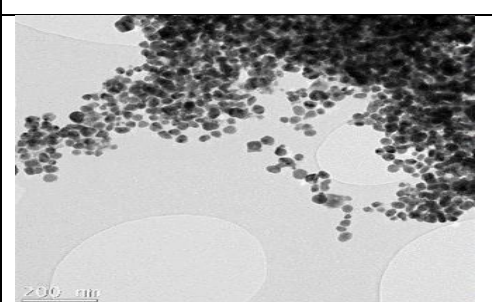
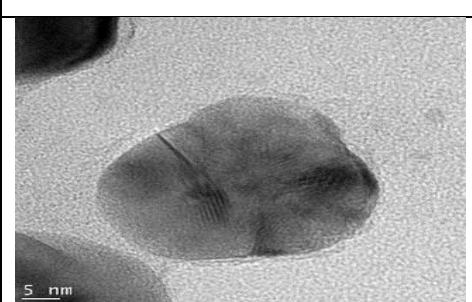
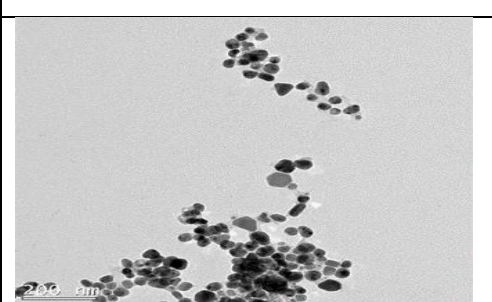
TEM images show only a few particles in each frame, hence statistically reliable distributions of these shapes and sizes cannot be evaluated using TEM [Zeiri et al. 2014]. Moreover, *Pistacia Atlantica* shows no apparent difference in Au NPs shapes at 25°C and 70°C. One interesting observation from the TEM images is the presence of a halo around some of the nanoparticles which could be revealing the biological layer on the nanoparticles caused by the phytochemicals and or proteins capping the metal nanoparticles. This halo around Au NPs synthesised from medicinal plant extracts was also observed by El-bagory et al., [2016]. This halo was also observed by Zeiri et al., [2014] which has a width of 2 to 3 nm, and was suggested to protect the Au NPs from aggregation.

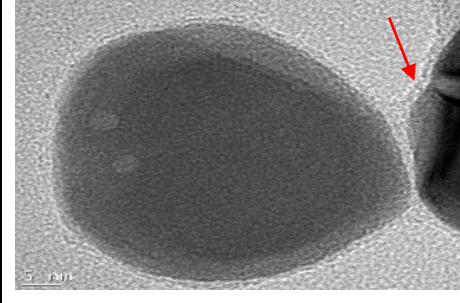
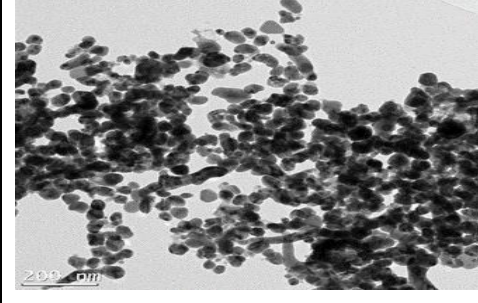
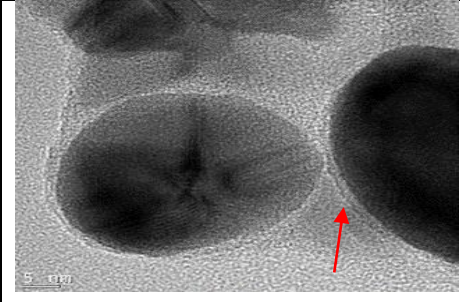
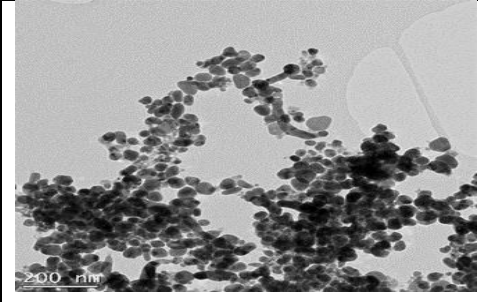
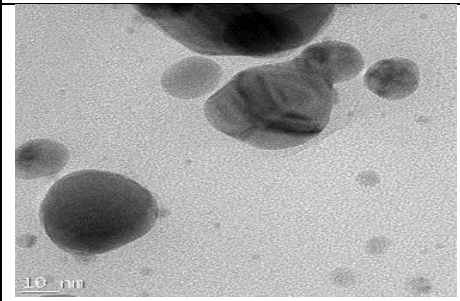
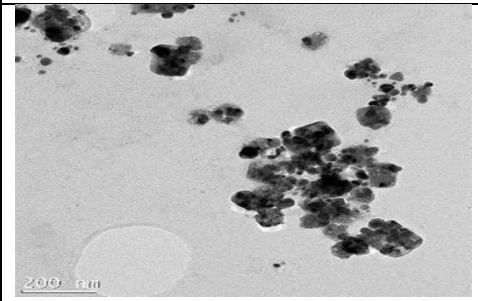
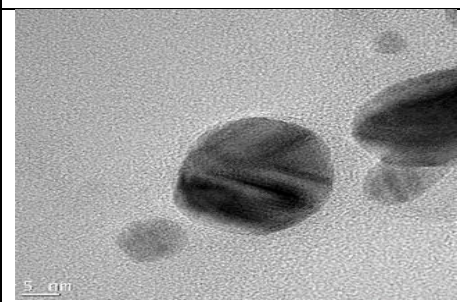
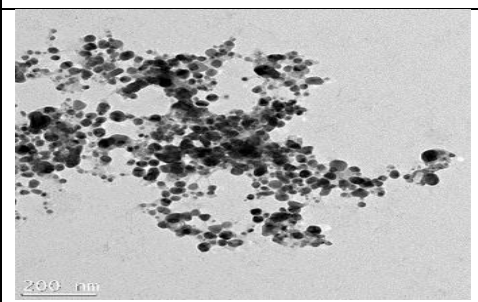
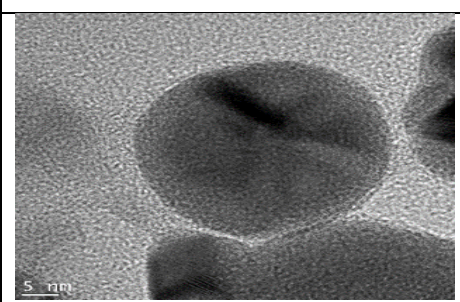
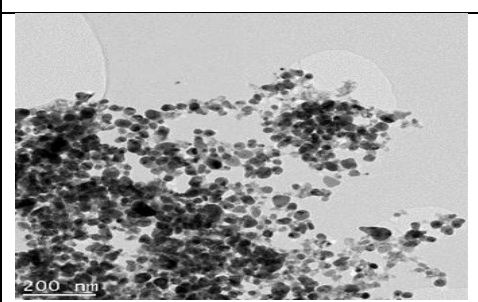
			
<i>P. atlantica at 25 °C</i>		<i>P. atlantica at 70 °C</i>	
			
<i>J. phoenicea at 25 °C</i>		<i>J. phoenicea at 70 °C</i>	
			
<i>T. capitatus at 25 °C</i>		<i>T. capitatus at 70 °C</i>	
			
<i>C. pubescens at 25 °C</i>		<i>C. pubescens at 70 °C</i>	

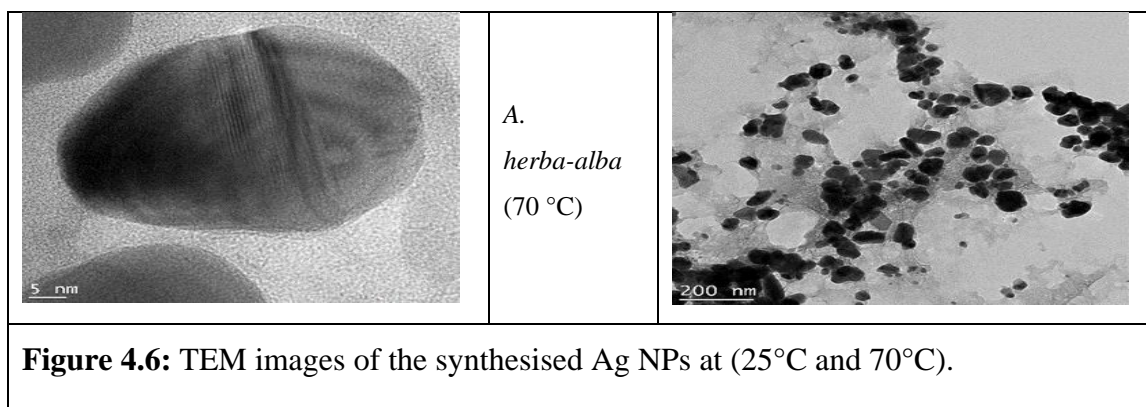


TEM images show that most silver nanoparticles synthesized at different concentrations of collected plant extracts are spherical. This can be seen in Figure 4.6. These spherical shapes are a common feature in Ag NPs as reported by Ahmed et al., [2016]. In Figure 4.6, the temperature of the synthesis reaction did not play a vital role in the shape and size of the nanoparticles, and it was observed that the nanoparticles at both low and high temperatures were close in shape and size. The dominant forms in both cases were the spherical form. It has been observed that silver nanoparticles synthesized with plant extracts are surrounded by a thin layer that may be from some organic matter [Shankar et al., 2004; Song and Kim 2009; Banerjee et al., 2014]. This aura can be seen in Figure 4.6 as indicated by red arrows.



	<p><i>P. atlantica</i> (70 °C)</p>	
	<p><i>J. phoenicea</i> (25 °C)</p>	
	<p><i>J. phoenicea</i> (70 °C)</p>	
	<p><i>R. officinalis</i> (25 °C)</p>	
	<p><i>R. officinalis</i> (70 °C)</p>	

	<p><i>T. capitatus</i> (25 °C)</p>	
	<p><i>T. capitatus</i> (70 °C)</p>	
	<p><i>G. alypum</i> (25 °C)</p>	
	<p><i>G. alypum</i> (70 °C)</p>	
	<p><i>A. herba-alba</i> (25 °C)</p>	



The Energy Dispersive X-ray analysis (EDS) spectroscopy analysis of the Au NPs confirmed the presence of gold and ions in the samples selected for TEM analysis. The presence of Au peaks in the spectrum confirming the synthesis of the gold nanoparticles (Figure 4.7). Strong Au optical adsorption peaks were observed at around 2.4, 9.7 and 11.5 KeV, which are consistent with a previous study [Arunachalam et al., 2013]. The presence of other strong peaks is due to the contribution of some of the extracts components in the solution and the characterization equipment, such as the copper grid. The presence of peaks for carbon, copper, and silicon in some samples is attributed to the TEM grid and the detector window, whereas the presence of calcium, oxygen, potassium, and chloride is suggested to be traced from the phytochemicals of the extracts [Zeiri et al., 2014].

EDS results reveal strong signal in the silver region and confirms the formation of silver nanoparticles which may have originated from the biomolecules bound to the surface of the silver nanoparticles (Figure 4.8). The presence of Ag peaks in the spectrum confirm the synthesis of Ag NPs. The EDS spectrum demonstrates a strong silver signal as well as weak signal oxygen, chloride, and carbon peak, which may have originated from the biomolecules associated with the surface of silver nanoparticles. Copper and carbon peaks may result from their presence in the same networks, suggesting that silver ions are reduced [Rodriguez-Leon et al., 2013; Rao et al., 2000]. In general, silver nanoparticles show a typical optical absorption peak of about 3 kV due to surface plasma resonance which is consistent with a previous study [Kotakadi et al., 2014]. There are no peaks for silver compounds observed. This determines that the silver compound has been fully reduced to Ag NPs as specified. While the 3 kV spectrum signal indicates a strong signal for nanoparticle particles [Sathishkumar et al., 2009].



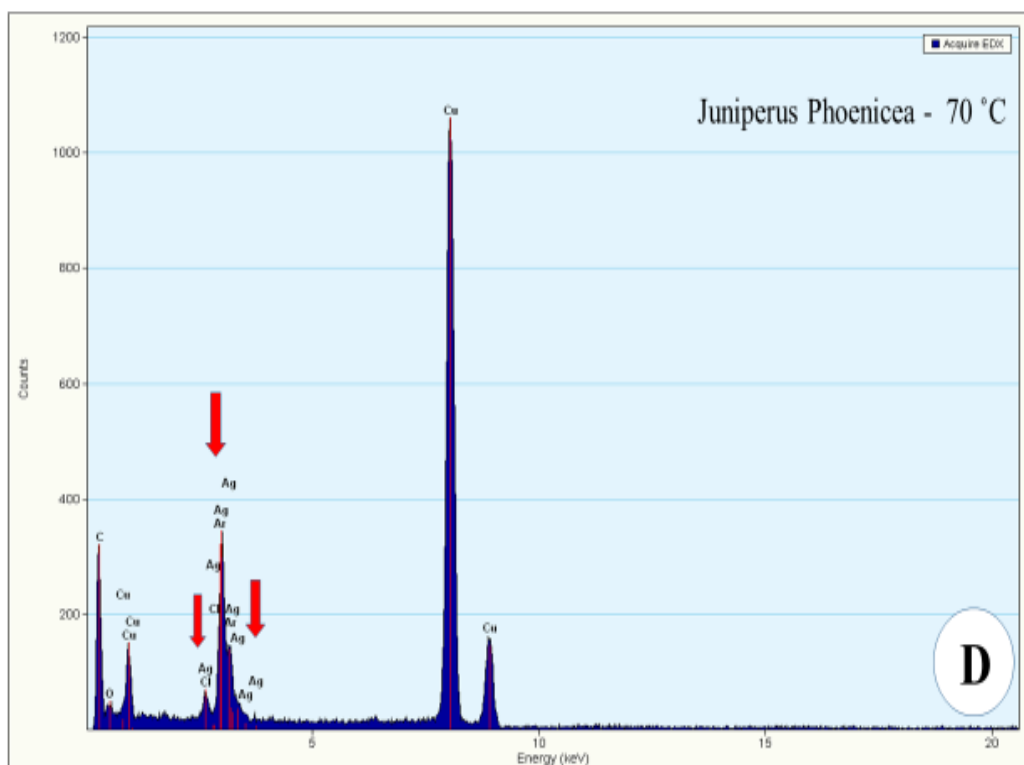
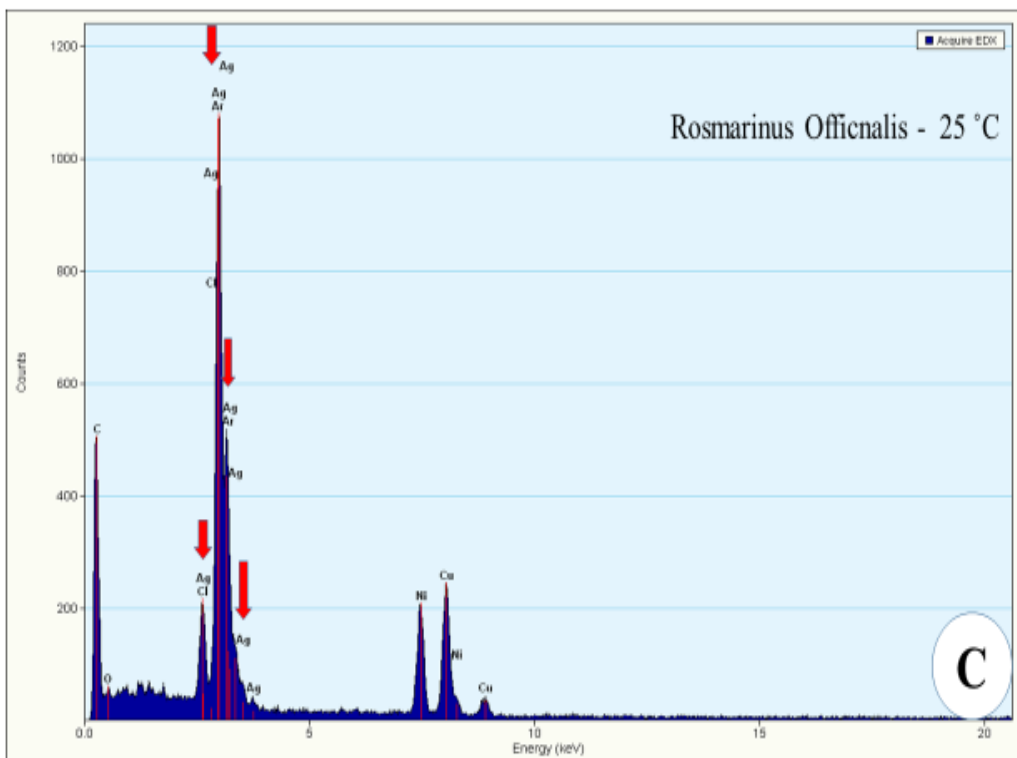


**Figure 4.8:** EDS spectra of Ag NPs synthesized from **C** (*R. officinalis* at 25 °C) and **D** (*J. phoenicea*, at 70 °C) showing Ag peaks in red arrows.

#### 4.2.4 Stability Assay

Studying the stability of the prepared nanoparticles is an important step to insure the effect of time on the structure and the functionality of the particles. Observations of zeta potential values of biosynthesized NPs have been carried out to assess their stability. In general, zeta potentials can be used to predict the long-term stability of NPs in a solution, where the volume of the charge reflects the forces of mutual antagonism between the particles [Chanda et al. 2011]. All plant extracts showed the potential of negative zeta potentials as shown in Tables 4.1 and 4.2 where it can be the cause of the nanoparticles stability in solutions. The biologically stable NPs (reflected by minimal changes in UV-Vis spectra) should not be clustered in a wide range of environmental conditions (eg, salts and biological additives). For further stability evaluation, the NPs were incubated for extended periods under different biological solutions. The results reveal good stability for some biosynthesized nanoparticles. This increases their potential in a biological application where we can conclude that their physical and chemical properties will be better preserved in the biological environment. It has been noted that the NPs remains stable in different biological media.

The stability of the NPs was monitored by recording ultraviolet spectra through different time periods. The Au NPs synthesized from *P. Atlantica* and *J. Phoenicea* were represented in Figure 4.9, no.1 and 8, While Ag NPs synthesized from *J. Phoenicea* and *R. officinalis* were represented in Figure 4.10, no.8 and 12, all of them showed excellent stability by maintaining surface plasmon resonance. This suggests that these nanoparticles are very stable in different environmental conditions and therefore can be used in various medical and calibration applications [Von-White et al. 2012]. On the other hand, none of the other NPs from other plant extracts showed similar stability at incubation with the same biological solutions.

Gold NPs synthesized from *A. graveolens* and *G. alypum* ; Ag NPs generated from *C. pubescens* and *S. officinalis* did not show the same simple changes in their respective UV spectra as shown in Figures 4.9 and 4.10, respectively. It is suggested that flattening in their SPR contributes to the formation of larger particles. During the incubation period, where their low intensity can also contribute to reducing the number of NPs. The researchers concluded that the proteins in the middle layer of NPs are stabilized and that the natural aura of NPs enhances their stability through possible interaction with media components in a way that is conducive to their stability [Sabuncum et al., 2012]. It can be observed that the size of NPs can

play a role in the interaction of NPs with the biological environment, leading to different observed results [Shang et al. 2014].

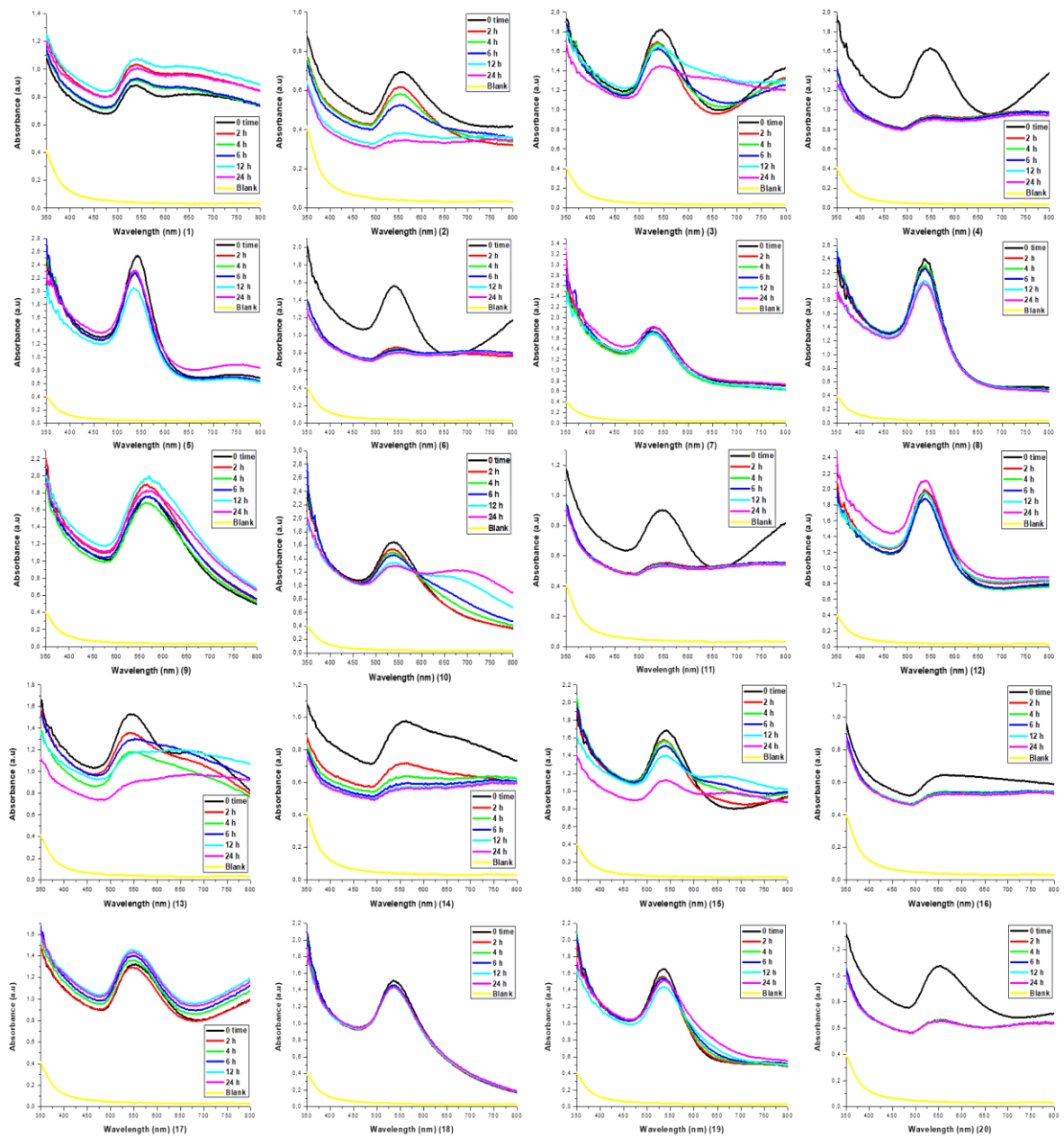


**Figure 4.9:** Stability assay of the Au NPs observed from uv-vis spectra after 24 h. upon incubation with nutrient broth media

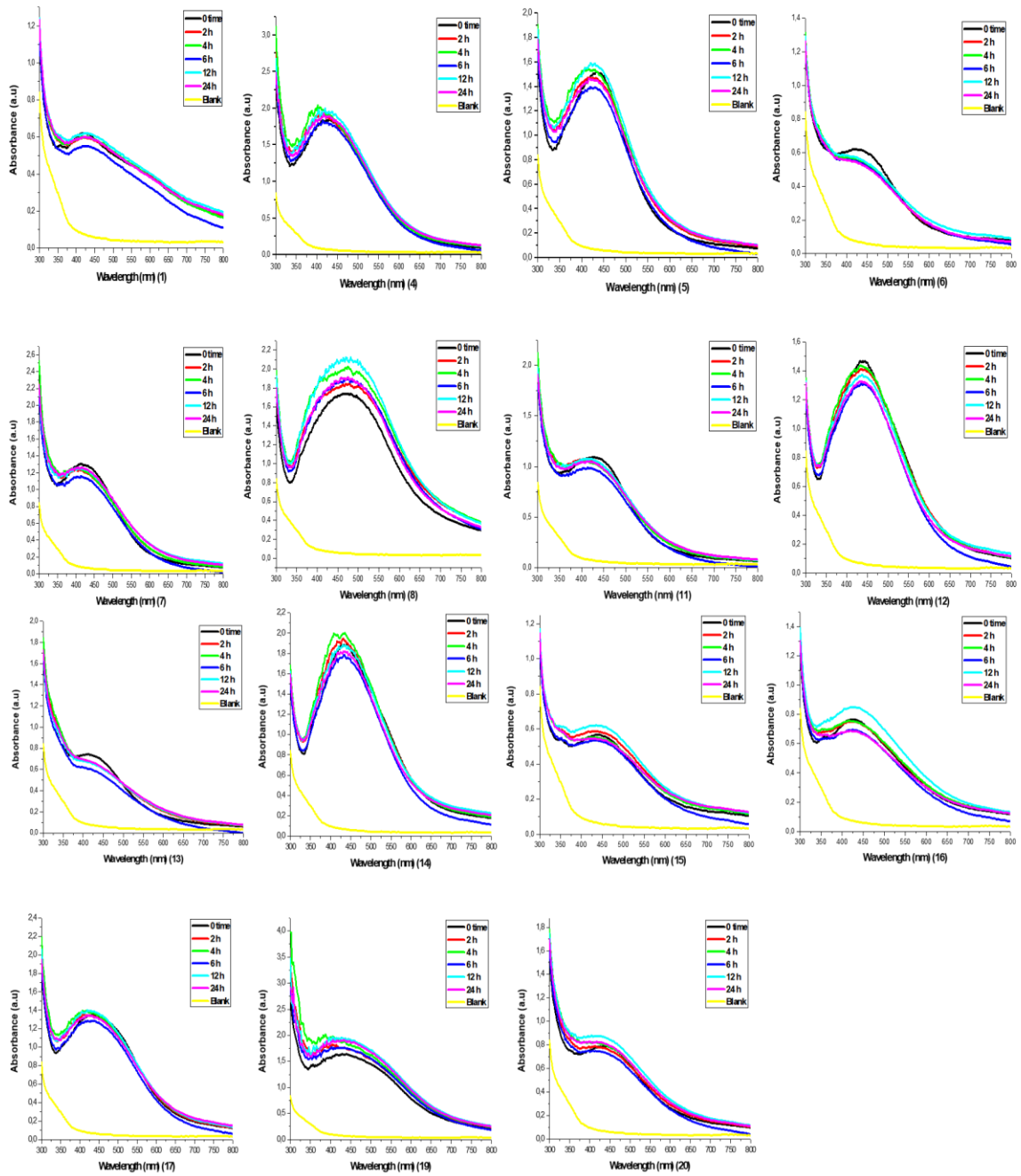


**Figure 4.10:** Stability assay of the Ag NPs observed from uv-vis spectra after 24 h. upon incubation with nutrient broth media

### 4.3 Selection of the effective plant extract(s)

Three plants were selected for further study. These are *P. atlantica*, *J. phoenicea*, and *R. officinalis*. The selection was done based on the TEM, UV, DLS stability results of the biosynthesized NPs using these plants extracts. The efficiency of these extracts was clear from the beginning where it shows rapid interaction, colour change which was initial confirmation of the formation of the NPs. The stability of the NPs synthesized from these extracts in the biological medium has been mentioned early. Further characterization will be reported to reveal the nature of these synthesized NPs as well as its activity in biological applications.

#### 4.3.1 X-ray diffraction (XRD)

XRD analysis was carried out to identify the crystallographic structure of the gold and silver NPs synthesized from the three selected plant extracts (*P. atlantica*, *J. phoenicea*, and *R. officinalis*). A smart lab diffractometer with a monochromatic  $\text{CuK}\alpha_1=1.5406 \text{ \AA}$  was used under operating voltage of 45 kV and a current of 200 mA in the Bragg-Brentano geometry. The biosynthesized nano-powder displays crystal clearly an amorphous signature. The four peaks corresponding to the standard gold and silver Bragg reflections (111), (200), (220), and (311) did not appear due to the amorphous nature of the prepared NPs [Krishnamurthy et al., 2014; Mehta et al., 2017].

#### 4.3.2 Kinetic study

The kinetics of the nanoparticles formation were studied by examining the changes in the  $\lambda_{\text{max}}$  of the plant extract/gold salt mixtures over 24 h. *P. atlantica* and *J. phoenicea*-NPs started to form and show  $\lambda_{\text{max}}$  above 1 Absorbance unit (AU) immediately with gold salt (Figure 4.6). This increase in  $\lambda_{\text{max}}$  is due to an increase in the number of NPs [Ahmad et al., 2003]. *P. atlantica* and *J. phoenicea*-NPs reached a maximum value after 60 min and then remained unchanged suggesting the reaction was complete at 60 min (Figure 4.11). On the other hand, for silver, the *J. phoenicea*, and *R. officinalis*-NPs started to change colour and the  $\lambda_{\text{max}}$  increased above 0.5 absorbance unit only after 40 min (Figure 4.12). Indicating the presence of lower reduction power phytochemicals in *J. phoenicea* and *R. officinalis*-NPs. The results in Figure 4.7 shows no constant  $\lambda_{\text{max}}$  after 1 h of incubation. Consequently, the full maturation of Ag NPs requires a minimum of 24 h.

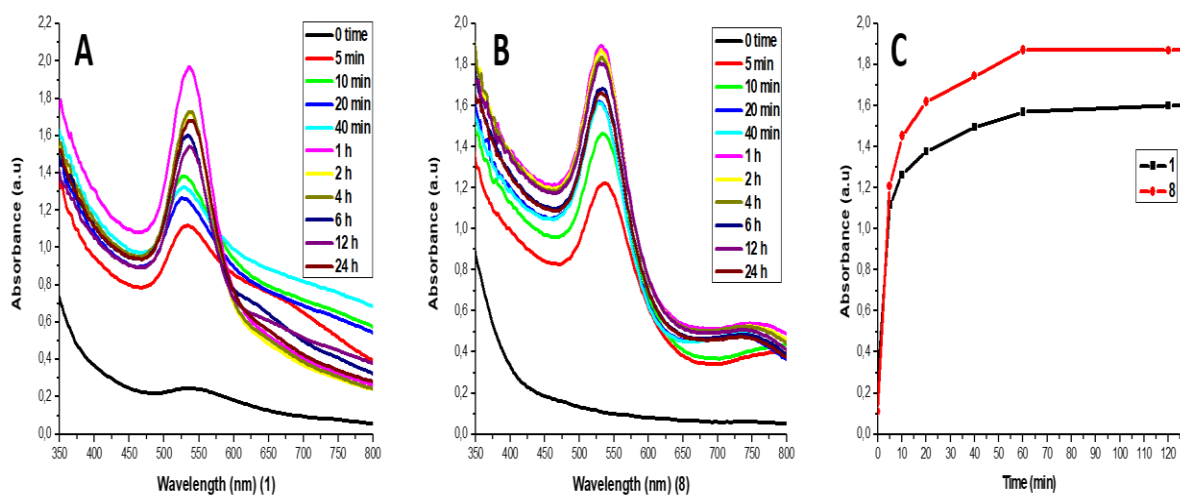


**Figure 4.11:** Kinetic study of Au NPs using (A) *P. atlantica*, (B) *R. officinalis* and (c)  $\lambda_{\max}$  values versus time

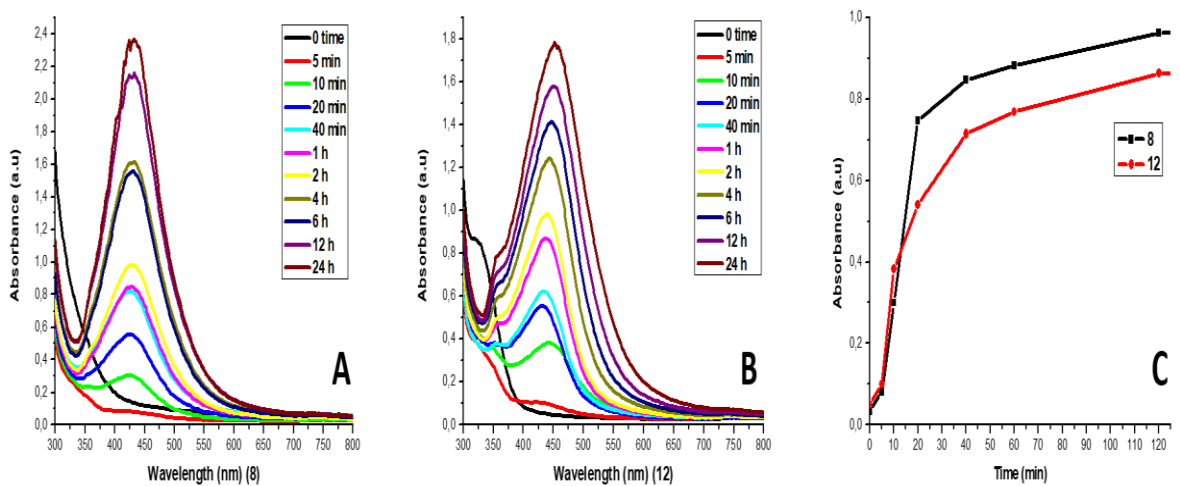


**Figure 4.12:** Kinetic study of Ag NPs via (A) *J. phoenicea*, (B) *R. officinalis* and (c)  $\lambda_{\max}$  values versus time

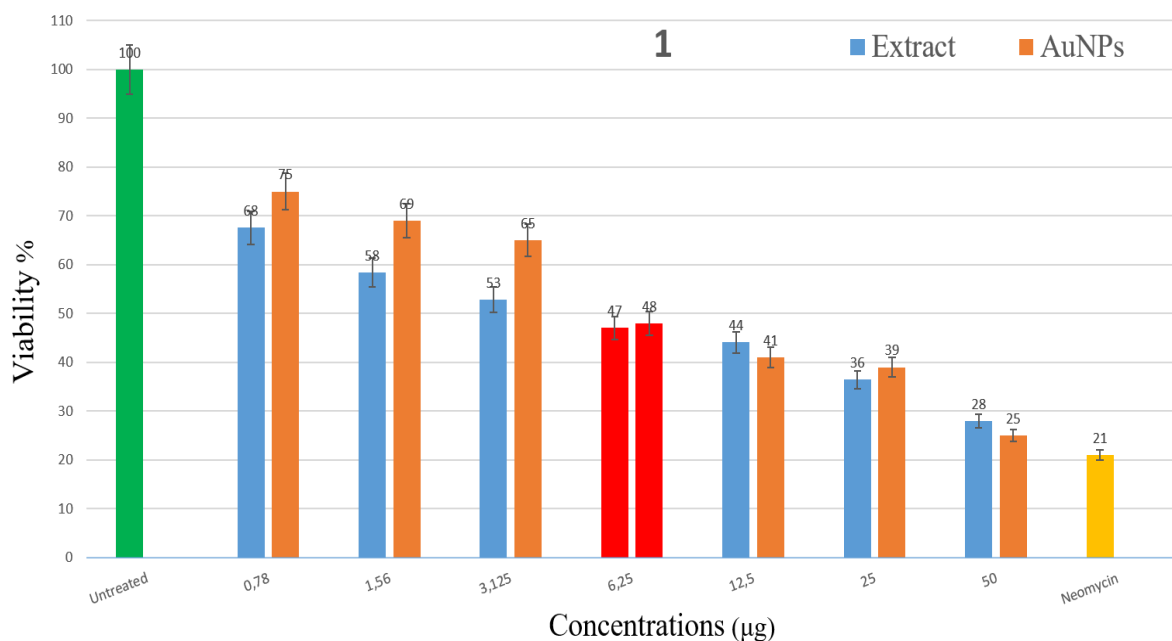
### 4.3.3 Evaluation of Antimicrobial activity of the gold and silver NPs

The antibacterial effect of various plant extracts is well documented and known. However, the antimicrobial effect of biosynthesized metallic NPs using plant extracts is still largely unexplored and could be useful as a new antibacterial agent [Shankar et al. 2004]. For this reason, antibacterial activities of the synthesized NPs from the selected plant extracts, *P. atlantica*, *J. phenicia*, and *R. officinalis*, have been investigated. Alamar blue (resazurin) was used to measure bacterial growth after treatment. Resazurin undergoes a change in chromatic response to reduce cellular metabolism to yield a highly fluorescent compound that can be quantified by measuring its fluorescence [Palombo 2011].

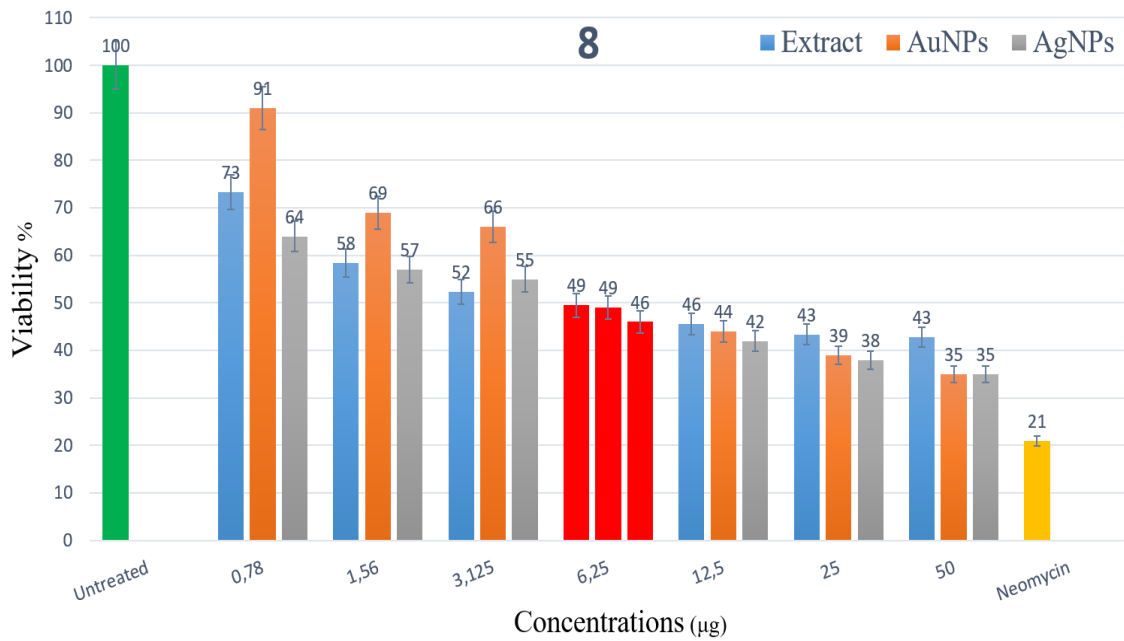
The minimum inhibitory concentration (MIC) ( $P < 0.05$ ) was known as the lowest concentration of tested samples inhibits the growth of tested bacterial strains compared to the value of negative control. Antibacterial evaluation was performed against the main cause of tooth decay, *S mutans*. The three selected plants extracts (*R. officinalis*, *J. phoenicea*, and *P. atlantica*) and the biosynthesized gold and silver NPs were tested. Neomycin antibody was used as a positive control. The results reveal different activity of the tested samples against *S mutans*. But what was interesting in Figures 4.13 and 4.14, *P. atlantica* extract and Au NPs synthesized *via* the same extract reveal same MIC value. Also, gold and silver NPs synthesized *via* *J. phoenicea* and the extract itself reveal similar MIC value.

Figure 4.15 shows slight differences in MIC values for the plant extract and its NPs, this may be due to the fact that bacteria adopt resistance mechanisms against free phytochemicals or that there is some synergistic activity between NPs and phytochemicals [Naimi & Khaled 2014]. This difference is also likely to be attributed to differences in the chemical nature of phytochemicals present in water extracts. The smaller size of NPs compared to the size of bacteria is thought to enable NPs to kill the bacterial cell by adhering to the cell wall [Abdulameer & Mahdi 2015]. NPs can then penetrate the cell wall of bacteria and induce death by influencing respiratory mechanisms and dividing cells by binding to compounds containing protein or phosphorus, such as DNA [De Haetano et al. 2015]. It is believed that the difference in activity against bacterial strains is dictated by the nature of the bacterial cell wall. i.e, the cell wall of the gram-positive germ strains contains an eptidoglycan nebula compared to the cell wall of gram negative bacteria [Huang et al. 2007]. As a result, the natural product / NPs conjugate can penetrate the cell wall of gram-negative bacteria and exert antibacterial activity more easily than gram-positive bacteria [Leela & Munusamy 2008].

Accordingly, the results showed that plant extracts had a bacterial activity at different concentrations tested in this study consistent with NPs. Antibacterial activity of the NPs can also be linked to an increase in the concentration of active phytochemicals that limit NPs. Thus, when bacteria are exposed to NPs, an enhanced antibacterial effect is obtained. It is also possible that the NPs are more targeted or closer to bacterial cells than free phytochemicals. Further support for the role of phytochemicals in inhibiting bacterial growth. Hence, we can speculate that the properties of phytochemicals that capping the NPs are an important factor in determining antibacterial activity regardless of the size of the NPs. Hence, *R. officinalis*, *J. phoenicea*, and *P. Atlantica* may be used in dental protection treatments for decay related problems.



**Figure 4.13:** Antibacterial activity of *P. atlantica* and its Au NPs, MIC's were represented by red color. Neomycin (yellow) was used as positive control.



**Figure 4.14:** Antibacterial activity of *J. phoenicea* and its Au, Ag NPs, MIC's were represented by red color. Neomycin (yellow) was used as positive control.

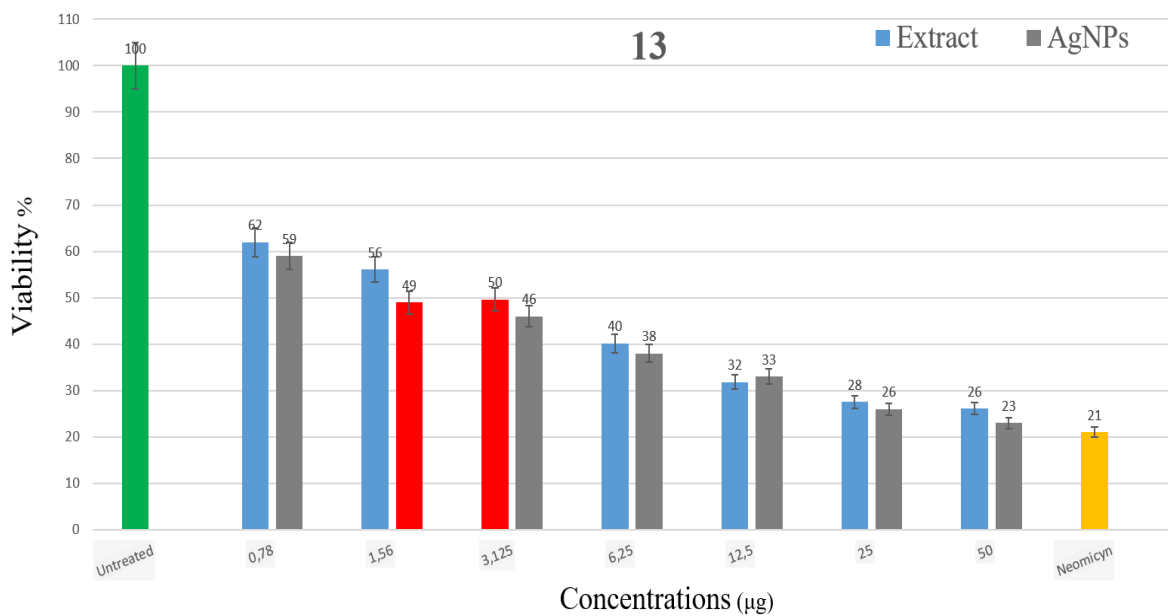


**Figure 4.15:** Antibacterial activity of *R. officinalis* and its Ag NPs, MIC's were represented by red color. Neomycin (yellow) was used as positive control.

# Chapter 5

## Conclusion and Future Prospects

Different plant extracts were successfully tested for their ability to synthesize NPs. Nanoparticles formation was tested in both temperature (25 °C and 70 °C). The optimal concentration of plant extract was determined for all 20 plants at each temperature.

The resultant NPs were characterized using uv-vis, DLS, HR-TEM and EDX. All four of these techniques confirmed the formation of colloidal NPs. The NPs formation and the physicochemical properties (size, charge, and shape) were dependent on several factors, include the chemical nature of plant constituents, the concentration of the extract, and the temperature, as well as incubation time

The DLS data showed that the Au NPs had an average diameter of 92 nm at 25 °C and 66 nm at 70 °C. The zeta potential values were observed to be negative for all the synthesized Au NPs , which corresponds to a negative surface charge of the nanoparticles and contributing to the stability of the Au NPs , and prevents aggregation. The HR-TEM showed the morphology and polydispersity, which reveals the uniformity of the synthesized Au NPs.

The Au NPs had shapes observed to be dominantly quasi-spherical and pentagonal respectively and also revealed the crystalline nature of the Au NPs. A halo surrounding the nanoparticle surface is also observed which possibly reveals the presence of a layer of biological material surrounding the nanoparticle.

The stability of all synthesized Au NPs was studied by incubating the Au NPs in nutrient broth prior to antibacterial evaluation. All the Au NPs under study showed stability, only minimal changes in the UV-Vis spectra of the Au NPs can be observed.

The antibacterial activity of *P. atlantica*, *J. phoenicea* plant extracts, and their respective Au NPs was studied using the microtiter method. The growth inhibition as demonstrated by the changes in the turbidity of the sample observed through optical density analysis was determined for each sample. Both Au NPs and their respective crude plant extracts showed significant dose-dependent antibacterial activity against *S. mutans*. It is probable that these nanoparticles possess an added pharmacological effect due to the phytochemicals capping the metallic nanoparticles. These nanoparticles have revealed promising bioactivity for developments of new antibacterial agents against *S. aureus* strains. It was observed that as the concentration of the Au NPs tested in this study increased, the antibacterial activity also increased demonstrating a dose-dependent activity of Au NPs.

These results showed that these two plant extracts and their respective Au NPs are potential antimicrobial agents against *S. mutans*. Their activity against other gram negative and gram positive bacterial strains and fungal species should be evaluated further, as well as its mechanisms of action. For applications in the development of antimicrobial agents, its toxicity must be investigated.

On the other hand, the DLS data of the synthesized Ag NPs showed that an average diameter of 58 nm at 25 °C and 91 at 70 °C. The zeta potential was observed to be negative for all the synthesized Ag NPs, which prevents aggregation. The HR-TEM showed the morphology and polydispersity. It has been observed that Ag NPs have approximately one shape. Where the spherical shape or spherical shape predominates over most of the domestic

product. A halo surrounding the nanoparticle surface as also observed which possibly reveals the presence of a layer of biological material surrounding the nanoparticle.

The stability of all synthesized Ag NPs was studied by incubating the Au NPs in nutrient broth prior to the antibacterial evaluation. All the Au NPs under study showed stability, only minimal changes in the UV-Vis spectra of the Ag NPs can be observed.

The antibacterial activity of *J. phoenicea*, *R. officinalis* plant extracts and their respective Ag NPs was studied using the microtiter method. The growth inhibition as demonstrated by the changes in the turbidity of the sample observed through optical density analysis was determined for each sample. Both Ag NPs and their respective crude plant extracts showed significant dose-dependent antibacterial activity against *S. mutans*. AgNPs are well known for their antibacterial activity, in this case the synthesised NPs may enhance the antibacterial of the capping agent and/or a kind of synergetic activity between them.

These nanoparticles have revealed promising bioactivity for developments of new antibacterial agents against *S. mutans* strains. It was observed that as the concentration of the Ag NPs tested in this study increased, the antibacterial activity also increased demonstrating a dose-dependent activity of Ag NPs.

These results show that these two plant extracts and their respective Ag NPs are potential antimicrobial agents against *S. mutans*. Their activity against other gram negative and gram positive bacterial strains and fungal species should be evaluated further, as well as its mechanisms of action. For applications in the development of antimicrobial agents, its toxicity must be investigated.

The field of green nanotechnology has opened great opportunities and possibilities, which bring hope to the pharmaceutical sector. Further optimization of synthesis and an in-depth characterization of these nanoparticles will lead to knowledge-based advancement in the

field of green nanotechnology. Different experimental conditions yield different nanoparticles in varying yields. Therefore, in line with the effort is being done towards the advancement of desired physicochemical properties which are towards establishing desired characteristics for various applications, optimal experimental conditions are crucial for obtaining desired characteristics and nanoparticle yield.

It is suspected that different phytochemicals are involved in synthesis. The synergistic effects of plant phytochemicals may play a key role in the bioactivity. More stable and potent formulations can also be explored by developing conjugates with the identified active phytochemicals which will probably confer increased stability of the active compounds or currently available antibiotics and increase their availability in the target site. These interactions and benefits are already expected from the synthesized nanoparticles and can be further enhanced to fit desired applications.

The analysis of the effect of these nanoparticles on various cells and the evaluation of their genotoxicity should be done to increase the understanding of their safety and increase their potential for biomedical applications. This will also give clear results when the nanoparticles are used in combination with other drugs for delivery or as part of combinatorial medicine as their effects will be fully understood. These studies will also give a clearer understanding of their sole therapeutic effects and mechanisms.

# References

- Abdel-Kader M.S. 2003. New ester and furocoumarins from the roots of *Pituranthos tortuosus*. *J Braz Chem Soc* 14(1), 48-51. doi.org/10.1590/S0103-50532003000100008.
- Abdulameer F.I. & Mahdi H.A. 2015. Investigation of *Streptococcus mutans* isolated from dental caries patients. *Mag Al-Kufa Univ Biol* 7.1, 50-63.
- Abdullah S.N.; Islam G.; Tabassum S.N. & Aslam M. 2018. Afsantin (*Artemisia absinthium* L.): a review. *World J Pharm Pharmaceut Sci* 7(12), 471-479. doi:10.20959/wjpps201812-12757.
- Ackerson C.J.; Jadzinsky P.D. & Kornberg R.D. 2005. Thiolate ligands for synthesis of water-soluble gold clusters. *J Am Chem Soc* 127, 6550–6551.
- Ahmad A.; Mukherjee P.; Senapati S.; Mandal D.; Khan M.I.; Kumar R. & Sastry M. 2003. Extracellular biosynthesis of silver nanoparticles using the fungus *Fusarium oxysporum*. *Colloids Surf B: Biointerf* 28.4, 313-318.
- Ahmed S.; Ahmad M.; Swami B.L. & Ikram S. 2016. A review on plants extract mediated synthesis of silver nanoparticles for antimicrobial applications: a green expertise. *J Adv Res* 7.1, 17-28.
- Akhtar, M.S.; Panwar J. & Yun Y.-S. 2013. Biogenic synthesis of metallic nanoparticles by plant extracts. *ACS Sustainable Chem Eng* 1(6), 591-602. doi.org/10.1021/sc300118u
- Al-Ahdab M.A. 2017. Hypoglycemic effect of alcoholic extracts of *Phyllanthus virgatus* and *Juniperus phoenicea* L., on streptozotocin-induced diabetic in male rats. *Life Sci J* 14(9), 61-70. doi:10.7537/marslsj140917.05.
- Al-Ali K.H.; Ibrahim N.A.; Ahmed A.A.; Hemeg H.A.; Abdelgawwad M.A. & Abdel-Salam H.A. 2017. Evaluation of the antimicrobial activities of *Cymbopogon schoenanthus* African. *J Microb Res* 11(17), 653-659. doi:10.5897/ajmr2017.8554.
- Alivisatos A.P.; Johnsson K.P.; Peng X.; Wilson T.E.; Loweth C.J. & Bruchez M.P. 1996. Jr Organization of 'nanocrystal molecules' using DNA. *Nature*. 382:609–11.

Al-Jawad S.; Taha, A.; Al-Halbosiy M. & Al-Barram L. 2018. Synthesis and characterization of small-sized gold nanoparticles coated by bovine serum albumin (BSA) for cancer photothermal therapy. *Photodiag Photodyn Ther* 21, 201-210.

Alomri A.A.; El Kloub F.K. & Moustafa N.E. 2018. Green synthesis of assembled silver nanoparticles in nano capsules of *Peganum harmala* L leaf extract. Antibacterial activity and conjugate investigation. *Cogent Chem* 4(1), 1532374/1-1532374/13. doi:10.1080/23312009.2018.1532374.

Al-Sheddi E.S.; Farshori N.N.; Al-Oqail M.M.; Al-Massarani S.M.; Saquib Q.; Wahab R.; Musarrat J.; Al-Khedhairi A.A.; & Siddiqui M.A. 2018. Anticancer potential of green synthesized silver nanoparticles using extract of *Nepeta deflersiana* against human cervical cancer cells (HeLA). *Bioinorg Chem Appl* 2018, ID 9390784, 12. doi.org/10.1155/2018/9390784.

Al-Yasiri A.Y.; Khoobchandani M.; Cutler C.S.; Watkinson L.; Carmack T.; Smith C.J.; Kuchuk M.; Loyalka S.K.; Lugão A.B. & Katti K.V. 2017. Mangiferin functionalized radioactive gold nanoparticles (MGF-198AuNPs) in prostate tumor therapy: green nanotechnology for production, in vivo tumor retention and evaluation of therapeutic efficacy. *Dalton Trans* 31; 46(42):14561-14571. doi: 10.1039/c7dt00383h.

Amin M.; Hameed S.; Ali A.; Anwar F.; Shahid S.A.; Shakir I.; Yaqoob A.; Hasan S.; Khan S.A.; Sajjad-Ur-Rahman. 2014. Green synthesis of silver nanoparticles: structural features and in vivo and in vitro therapeutic effects against *Helicobacter pylori* induced gastritis. *Bioinorg Chem Appl* 135824/1-135824/11, 12 pp.. doi:10.1155/2014/135824.

Amri O.; Zekhnini A.; Bouhaimi A.; Tahrouch S. & Hatimi A. 2018. Anti-inflammatory activity of methanolic extract from *Pistacia atlantica* Desf. Leaves. *Pharmacog J* 10(1), 71-76. doi:10.5530/pj.2018.1.14.

Andor B.; Tischer A.A.; Berceanu-Vaduva D.; Lazureanu V.; Cheveresan A. & Poenaru M. 2019. Antimicrobial activity and cytotoxic effect on gingival cells of silver nanoparticles obtained by biosynthesis. *Revista de Chimie*, 70(3), 781-783.

Appenzeller T. 1991. The man who dared to think small. *Science* 254:1300.

Arassu R. R.; Nambikkairaj B. & Ramya D. R. 2018. Synthesis of silver nanoparticles and characterization using plant leaf essential oil *Rosemarinus officinalis* and their antifungal

activity against human pathogenic fungi. *J Sci Res Phar* 7(11), 138-144. doi:10.5281/zenodo.1489509.

Arunachalam K.D.; Sathesh K.A. & Shanmugasundaram H. 2013. One-step green synthesis and characterization of leaf extract-mediated biocompatible silver and gold nanoparticles from *Memecylon umbellatum*. *Int J Nanomedicine* 8, 1307.

Ashraf S.S.; Islam N.; Iqbal A.; Sheeraz M.; Quraishi H.A. & Rather S.A. 2019. *Artemisia absinthium* linn (Afsanteen): a review. *World J Phar Pharmaceut Sci* 8(1), 1421-1427. doi:10.20959/wjpps20191-13042.

Atiyeh B.S.; Costagliola M.; Hayek S.N. & Dibo S.A. 2007. Effect of silver on burn wound infection control and healing: review of the literature. *Burns* 33:139–48.

Awad M.A.; Hendi A.A.; Ortashi K.M.; Aldalbahi A.K. & Alnamlah R.A. 2019. Synthesis of zinc oxide nanoparticles using *cymbopogon proximus* extract from U.S. US 10358356 B1 20190723.

Azizi M.; Sedaghat S.; Tahvildari K.; Derakhshi P. & Ghaemi A. 2017. Synthesis of silver nanoparticles using *Peganum harmala* extract as a green route. *Green Chem Lett Rev* 10(4), 420-427., doi:10.1080/17518253.2017.1395081.

Bagheri S.; Sarabi M.; Moradi K.; Peyman K.; Reza M.; Veiskarami S.; Ahmadvand H. & Keshvari M. 2019. Effects of *Pistacia atlantica* on Oxidative Stress Markers and Antioxidant Enzymes Expression in Diabetic Rats. *J Am Coll Nutr* 38(3), 267-274. doi:10.1080/07315724.2018.1482577.

Banerjee P.; Satapathy M.; Mukhopahayay A. & Das P. 2014. Leaf extract mediated green synthesis of silver nanoparticles from widely available Indian plants: synthesis, characterization, antimicrobial property and toxicity analysis. *Bioresour Bioprocess* 1.1, 3. doi.org/10.1186/s40643-014-0003-y.

Baptista P.; Pereira E.; Eaton P.; Doria G.; Miranda A.; Gomes I.; Quaresma P.; Franco R. 2007. Gold nanoparticles for the development of clinical diagnosis methods. *Anal Bioanal Chem* 391, 943-950.

Ben Othman M.; Neffati M. & Isoda H. 2017. Anti-stress effects of Tunisian *Cymbopogon schoenanthus* L. ethanol extract and some of its active compounds. *J Agr Sci Techn A*, 7(2), 91-99. doi:10.17265/2161-6256/2017.02.003.

- Bolaños K.; Kogan M.J.; & Araya E. 2019. Capping gold nanoparticles with albumin to improve their biomedical properties. *Int J Nanomed* 14: 6387–6406. doi: 10.2147/IJN.S210992.
- Bouassida K.Z.; Makni S.; Tounsi A.; Jlaiel L.; Trigui M. & Tounsi S. 2018. Effects of *Juniperus phoenicea* hydroalcoholic extract on inflammatory mediators and oxidative stress markers in carrageenan-induced paw oedema in mice. *Bio Med Res. Int* 3785487/1-3785487/11. doi:10.1155/2018/3785487.
- Boudjelal A. Siracusa L.; Henchiri C.; Sarri M.; Abderrahim B.; Baali F. & Ruberto G. 2015. Antidiabetic effects of aqueous infusions of *Artemisia herba-alba* and *Ajuga iva* in alloxan-induced diabetic rats *Planta Med* 81(9), 696-704 doi:10.1055/s-0035-1546006.
- Boulos, L. 1971. The flora of Libya project. *Mitt. Bot. Staatssamml. München* 10, 14-16.
- Boussoualim N.; Trabsa H.; Krache I.; Arrar L. & Baghiani A. 2016. Kinetics of inhibition of xanthine oxidase by *globularia alypum* and its protective effect against oxonate-induced hyperuricemia and renal dysfunction in mice. *J Appl Pharmaceut Sci* 6(4), 159-164. doi:10.7324/JAPS.2016.60422.
- Brown K.R.; Natan M.J. 1998. Hydroxylamine seeding of colloidal Au nanoparticles in solution and on surfaces. *Langmuir*. 14:726–8.
- Cele L.M.; Suprakas S.R. & Neil J. C. 2009. Nanoscience and nanotechnology in South Africa. *South Afr J Sci* 105.7-8: 242-242.
- Chanda N.; Shukla R.; Zambre A.; Mekapothula S.; Kulkarni R.R.; Katti K.; et al., 2011. An effective strategy for the synthesis of biocompatible gold nanoparticles using cinnamon phytochemicals for phantom CT imaging and photoacoustic detection of cancerous cells. *Pharm Res* 28(2):279-91. doi: 10.1007/s11095-010-0276-6.
- Chen R.; Wu J.; Li H.; Cheng G.; Lu Z. & Che C. 2010. Fabrication of gold nanoparticles with different morphologies in HEPES buffer. *Rare Metals* 29, 180-186.
- Dahl J.A., Maddux B.L.S. and Hutchison J.E. 2007. Toward greener nanosynthesis. *Chem Rev* 107 2228-2269.
- De Gaetano F.; Ambrosio L.; Raucci M.G.; Marotta A. & Catauro M. 2005. Sol-gel processing of drug delivery materials and release kinetics. *J Mater Sci Mater Med* 16(3):261-5. doi: 10.1007/s10856-005-6688-x.

- Dong, X.; Ji X.; Wu H.; Zhao L.; Li J. & Yang W. 2009. Highly efficient multicolor up-conversion emissions and their mechanisms of monodisperse NaYF<sub>4</sub>:Yb, Er core and core/shell-structured nanocrystal. *J Phys Chem C* 113, S1-S3
- Dzimitrowicz, A.; Berent, S.; Motyka, A.; Jamroz, P.; Kurcbach, K.; Sledz, W.; & Pohl, P. (2019). Comparison of the characteristics of gold nanoparticles synthesized using aqueous plant extracts and natural plant essential oils of *Eucalyptus globulus* and *Rosmarinus officinalis*. *Arab J Chem* 12(8), 4795-4805.
- El-Dahmy S.I. 1993. Further benzofuran derivatives and the antiinflammatory activity of *Helichrysum stoechas* (L.) grown in Libya. *Zagazig J Pharmaceut Sci* 2(1), 73-80.
- El-Sayed I.H.; Huang X.; El-Sayed M.A. 2005. Surface plasmon resonance scattering and absorption of anti-EGFR antibody conjugated gold nanoparticles in cancer diagnostics: applications in oral cancer. *Nano Lett.* 5:829.
- Erdogan O.; Abbak M.; Demirbolat G.M.; Birtekocak F.; Aksel M.; Pasa S. et al. 2019. Green synthesis of silver nanoparticles via *Cynara scolymus* leaf extracts: The characterization, anticancer potential with photodynamic therapy in MCF7 cells. *PLoS ONE* 14(6): e0216496. <https://doi.org/10.1371/journal.pone.0216496>.
- Featherstone J.D. 1999. Prevention and reversal of dental caries: Role of low level fluoride. *Community Dent Oral Epidemiol* 27(1):31-40.
- Foss C.; Hornyak G.; Stockert J.; Martin C. 1994. Template-synthesized nanoscopic gold particles: optical spectra and the effects of particle size and shape. *J Phys Chem* 98, 2963-2971.
- Frens G. 1972. Particle size and sol stability in metal colloids. *Coll Polym Sci* 250:736-41.
- Ge Y.; Gu N.; Ma W.; Zhang Y.; Zhou X.; Zhao Y.; Zhou H.; Huang Z.; Guo D.; Wu J.; Zhang X. & Zhu L. 2013. *Biomater* 34, 7884-7894.
- Ghlassi Z.; Krichen F.; Kallel R.; Amor I.; Boudawara T.; Gargouri J.; Zeghal K.; Hakim A.; Bougatef A. & Sahnoun, Z. 2019. Sulfated polysaccharide isolated from *Globularia alypum* L.: Structural characterization, *in vivo* and *in vitro* anticoagulant activity, and toxicological profile. *Int J Biol Macromol* 123, 335-342. doi:10.1016/j.ijbiomac.2018.11.044.
- Goel S.; England C.G.; Chen F. & Cai W. 2017. Positron emission tomography and nanotechnology: A dynamic duo for cancer theranostics. *Adv Drug Deliv Rev* 113, 157-176.

Goud B.J. & Poornima D. 2018. Role of *Artemisia absinthium* on lipid peroxidation in the brain tissues of STZ lured diabetic rats. *Int J Pharm Pharmaceut Res* 13(3), 61-71.

Guo D.; Zhang J.; Huang Z.; Jiang S. & Gu N. 2015. Colloidal silver nanoparticles improve anti-leukemic drug efficacy via amplification of oxidative stress. *Colloid Surf B: Biointerfaces*. 126. 10.1016/j.colsurfb.2014.12.023.

Hajjaj G.; Chakour R; Bahlouli A; Tajani M; Cherrah Y & Zellou A. 2018. Evaluation of CNS activity and anti-inflammatory effect of *Pistacia atlantica* desf. essential oil from Morocco. *Pharmaceut Chem J* 5(3), 86-94.

Hajji N.; Jabri M.; Tounsi H.; Wanes D.; Ben El Hadj A.I.; Boulila A.; Marzouki L. & Sebai H. 2018. Phytochemical analysis by HPLC-PDA/ESI-MS of *Globularia alypum* aqueous extract and mechanism of its protective effect on experimental colitis induced by acetic acid in rat. *J Funct Foods* 47, 220-228. doi:10.1016/j.jff.2018.05.058.

Hamada S. & Slade H.D. Biology, immunology, and cariogenicity of *Streptococcus mutans*. *Microbiol Rev* 1980; 44(2):331-384.

Hamedani Y.P. & Hekmati M. 2019. Green biosynthesis of silver nanoparticles decorated on multi-walled carbon nanotubes using the extract of *Pistacia atlantica* leaves as a recyclable heterogeneous nanocatalyst for degradation of organic dyes in water. *Polyhedron* 164, 1-6. doi:10.1016/j.poly.2019.02.010.

Hasan H.M. & Ali A.M. 2017. Separation and identification the speciation of the phenolic compounds in fruits and leaves of some medicinal plants (*Juniperus phoenicea* and *Quercus coccifera*) growing at Al -Gabal Al -Akhder region (Libya). *Ind J Pharmaceut Educ Res* 51(3, Suppl. 1), S299-S303. doi:10.5530/ijper.51.3s.34.

Hashim G.M.; Almasaudi S.B.; Azhar E.; Al Jaouni S.K.; & Harakehb S. 2017. Biological activity of *Cymbopogon schoenanthus* essential oil. *Saudi j biolog sci* 24(7), 1458–1464. doi:10.1016/j.sjbs.2016.06.001.

Hayat M.A. 1989. Colloidal gold: principles, methods, and applications. San Diego: Academic Press.

Holmberg K. 2003. Organic reactions in microemulsions. *Curr Opin Colloid Interface Sci.* 8, 145-155.

- Huang J.; Li Q.; Sun D.; Lu Y.; Su Y.; Yang X.; ... Chen C. 2007. Biosynthesis of silver and gold nanoparticles by novel sun dried *Cinnamomum camphora* leaf. *Nanotechnology* 18(10), 105104. doi:10.1088/0957-4484/18/10/105104.
- Iravani, S. 2011. Green synthesis of metal nanoparticles using plants. *Green Chem* 13.10: 2638-2650.
- Isaac R.S., Sakthivel G., & Murthy C.H. 2013. Green synthesis of gold and silver nanoparticles using *Averrhoa bilimbi* fruit extract. *J Nanotechnol* (2013). ID 906592. doi.org/10.1155/2013/906592.
- Jana N.R.; Gearheart L. & Murphy C.J. 2001a. Wet chemical synthesis of high aspect ratio cylindrical gold nanorods. *J Phys Chem B*. 105:4065–7.
- Jana N.R.; Gearheart L.; Murphy C.J. 2001b. Seed-mediated growth approach for shape-controlled synthesis of spheroidal and rod-like gold nanoparticles using a surfactant template. *Adv Mater* 13:1389–93.
- Jana S.; Kondakova A.V. ; Shevchenko S.N.; Sheval E.V.; Gonchar K.A.; Timoshenko V.Y.; Vasiliev A.N. 2017. Halloysite nanotubes with immobilized silver nanoparticles for anti-bacterial application. *Colloid Surf B Biointerface* 151: 249–254.
- Jeyaraj M.; Sathishkumar G.; Sivanandhan G.; Mubarak A.; Rajesh M.; Arun R.; Kapildev G. ; Manickavasagam M.; Thajuddin N.; Premkumar K.; & Ganapathi A. 2013. Biogenic silver nanoparticles for cancer treatment: an experimental report. *Coll Surf B Biointerface* 106, 86–92.
- Joerger R.; Klaus T. & Granqvist C.G. 2000. Biologically produced silver–carbon composite materials for optically functional thin-film coatings. *Adv Mater* 12.6; 407-409.
- Jung S.H.; Kim K.I.; Ryu J.H.; Choi S.H.; Kim J.B.; Moon J.H. & Jin J.H. 2010. Preparation of radioactive core–shell type  $^{198}\text{Au}@ \text{SiO}_2$  nanoparticles as a radiotracer for industrial process applications. *Appl Radiat Isot* 68, 1025–1029.
- Kadri, M.; Salhi, N.; Yahia, A.; Amiar, K. & Ghabziah, H. 2017. Chemical composition, antioxidant and antimicrobial activities from extracts of *Cymbopogon schoenanthus* L. (Spreng) of Algeria. *Int J Biosci* 10(1), 318-326. doi:10.12692/ijb/10.1.318-326.
- Kang Y.S.; Risbud S.; Rabolt J.F. & Stroeve P. 1996. Synthesis and characterization of nanometer-size  $\text{Fe}_3\text{O}_4$  and  $\gamma\text{-Fe}_2\text{O}_3$  particles. *Chem Mater*. 8:2209–11.

- Khoobchandani M.; Katti K.; Maxwell A.; Fay W.P. & Katti KV. 2016. Laminin receptor-avid nanotherapeutic egcg-aunps as a potential alternative therapeutic approach to prevent restenosis. *Int J Mol Sci* 17(3): 316. doi: 10.3390/ijms17030316.
- Kotakadi V.S.; Gaddam S.A.; Subba R.Y.; Prasad T.N.; Varada R. & Sai Gopal D.V. 2014. Biofabrication of silver nanoparticles using *Andrographis paniculata*. *Eur J Med Chem* 12;73:135-40. doi: 10.1016/j.ejmech.2013.12.004.
- Kraza, L.; Mourad, S. M. & Halis, Y. 2019. Anti-fungal and antibacterial effects of *Globularia alypum* L. extracts and their antioxidant activities. *J Chem Pharmaceut Res* 11(2), 68-77.
- Krishnamurthy S.; Esterle A.; Sharma N. & Sahi S.V. 2014. Yucca-derived synthesis of gold nanomaterial and their catalytic potential. *Nanoscale Res Lett* 23;9(1):627. doi: 10.1186/1556-276X-9-627.
- Lansdown A.B. 2006. Silver in health care: antimicrobial effects and safety in use. *Curr Probl Dermatol*. 33:17–34.
- Lee P.C. & Meisel D. 1982. Adsorption and surface-enhanced raman of dyes on silver and gold sols *J. Phys. Chem.* 86, 3391-3395.
- Leela A. & Vivekanandan M. 2008. Tapping the unexploited plant resources for the synthesis of silver nanoparticles. *Afr J Biotechnol* 7.17.
- Les, F.; Venditti, A.; Casedas, G.; Frezza, C.; Guiso, M.; Sciubba, F.; Serafini, M.; Bianco, A.; Valero, M.S. & Lopez, V. 2017. Everlasting flower (*Helichrysum stoechas* Moench) as a potential source of bioactive molecules with antiproliferative, antioxidant, antidiabetic and neuroprotective properties. *Ind Crops Prod* 108, 295-302. doi:10.1016/j.indcrop.2017.06.043.
- Liu J.; He K.; Wu W.; Song T.B.; Kanatzidis M.G. 2017. *In situ* synthesis of highly dispersed and ultrafine metal nanoparticles from chalcogels. *J Am Chem Soc* 1;139(8):2900-2903. doi: 10.1021/jacs.6b13279.
- Lukman A.I. Gong B.; Marjo CE.; Roessner U & Harris A.T. 2011. Facile synthesis, stabilization, and anti-bacterial performance of discrete Ag nanoparticles using *Medicago sativa* seed exudates. *J Colloid Interface Sci* 15;353(2):433-44. doi: 10.1016/j.jcis.2010.09.088.

- Mackey B.K.; & El-Sayed, M.A. 2010. Nuclear targeting of gold nanoparticles in cancer cells induces DNA damage, causing cytokinesis arrest and apoptosis. *J Am Chem Soc* 132, 5, 1517-1519. <https://doi.org/10.1021/ja9102698>.
- Maeh K.; Jaaffar I. & AL-azawi K.F. 2019. Preparation of *juniperus* extract and detection of its antimicrobial and antioxidant activity. *Iraqi J Agric Sci* 50(4): 1153-1161.
- Mahjoub F.; Akhavan R.K.; Yousefi M.; Mohebbi M.; & Salari R. 2018. *Pistacia atlantica* Desf. A review of its traditional uses, phytochemicals and pharmacology. *J med life*, 11(3), 180–186. doi:10.25122/jml-2017-0055.
- Medjeldi S.; Bouslama L.; Benabdallah A.; Essid R.; Haou S. & Elkahoui S. 2018. Biological activities, and phytochemicals of northwest Algeria *Ajuga iva* (L) extracts: Partial identification of the antibacterial fraction. *Microb Pathogen* 121, 173-178. doi:10.1016/j.micpath.2018.05.022.
- Mehta B.K.; Meenal Chhajlani & Shrivastava B.D. 2017. Green synthesis of silver nanoparticles and their characterization by XRD” *J Phy: Conf Series* 836;012050 doi:10.1088/1742-6596/836/1/012050.
- Mighri H.; Sabri K.; Eljeni H.; Neffati M. & Akrou A. 2015. Chemical composition and antimicrobial activity of *Pituranthos chloranthus* (Benth.) Hook and *Pituranthos tortuosus* (Coss.) Maire essential oils from southern Tunisia. *Adv Biol Chem* 5, 273-278.
- Miri M.R.; Khosravi R.; Taghizadeh A.A.; Fazlzadehdavil M.; Samadi Z.; Eslami H. Gholami A.; Ghahramani E. 2019. Comparison of zero valent iron and zinc oxide green nanoparticles loaded on activated carbon for efficient removal of Methylene blue. *Desal Water Treat* 148, 312-323. doi:10.5004/dwt.2019.23883.
- Mody V.V., Nounou M.I., Bikram M. 2009. Novel nanomedicine-based MRI contrast agents for gynecological malignancies. *Adv Drug Deliv Rev* 61:795–807.
- Molaie, R.; Farhadi, K.; Forough, M. & Hajizadeh, S. 2018. Green biological fabrication and characterization of highly monodisperse palladium nanoparticles using *Pistacia atlantica* fruit broth. *J Nanostruct* 8(1), 47-54. doi:10.22052/jns.2018.01.006.
- Moloudizargari M.; Mikaili P.; Aghajanshakeri S.; Asghari M. H. & Shayegh J. 2013. Pharmacological and therapeutic effects of *Peganum harmala* and its main alkaloids. *Pharmaco Rev* 7(14), 199–212. doi:10.4103/0973-7847.120524.

- Moustafa N.E. & Alomari A.A. 2019. Green synthesis and bactericidal activities of isotropic and anisotropic spherical gold nanoparticles produced using *Peganum harmala* L. leaf and seed extracts. *Biotechn Appl Bioch* 66(4), 664-672.
- Murphy C.J.; Gole A.M.; Stone J.W.; Sisco P.N.; Alkilany A.M.; Goldsmith E.C.; et al. 2008. Gold nanoparticles in biology: beyond toxicity to cellular imaging. *Acc Chem Res* 41:1721–30.
- Murugesan K.; Koroth J.; Srinivasan P.P.; Singh A.; Mukundan S.; Karki S.S.; Choudhary B. & Gupta C.M. 2019. Effects of green synthesised silver nanoparticles (ST06-AgNPs) using curcumin derivative (ST06) on human cervical cancer cells (HeLa) in vitro and EAC tumor bearing mice models. *Int J Nanomed* 14, 5257—5270.
- Naimi, M. & Khaled M.B. 2014. Exploratory tests of crude bacteriocins from autochthonous lactic acid bacteria against food-borne pathogens and spoilage bacteria exploratory tests of crude bacteriocins from autochthonous lactic acid bacteria against food-borne pathogens and spoilage bact. *World Acad. Sci. Eng Technol* 8, 113-119.
- Nancy B.A. & Elumalai K. 2019. Synthesis of silver nanoparticles using *Rosmarinus officinalis* leaf oil and its antimicrobial activity against vaginal candidiasis. *Int J Pharm Biolog Sci* 9(1), 233-241. doi:10.21276/ijpbs.2019.9.1.30.
- Palombo E.A. 2011. Traditional medicinal plant extracts and natural products with activity against oral bacteria: Potential application in the prevention and treatment of oral diseases. *Evid-Based Complem Alter Med* 2011: 680354.
- Parashar V.; Parashar R.; Sharma B. & Pandey AC. Parthenium leaf extract mediated synthesis of silver nanoparticles: a novel approach towards weed utilization. *Digest J Nanomat Biostruc* 4(1):45-50.
- Park H.; Hwang Y.H.; Kim D.G.; Jeon J. & Ma J.Y. 2015. Hepatoprotective effect of herb formula KIOM2012H against nonalcoholic fatty liver disease. *Nutrients* 2;7(4):2440-55. doi: 10.3390/nu7042440.
- Radford, E.; Gianluca C.A. & de Montmollin B. 2011. Important plant areas of the south and east Mediterranean region: priority sites for conservation. No. 333.950916384 I34. IUCN Gland (Suiza) WWF, Gland (Suiza).

Rajkuberan C.; Prabukumar S.; Sathishkumar G.; Wilson A.; Ravindran K. & Sivaramakrishnan S. 2017, Facile synthesis of silver nanoparticles using *Euphorbia antiquorum* L. latex extract and evaluation of their biomedical perspectives as anticancer agents. *J Saudi Chem Soc* 21, 8, 911-919.

Rao R.C.; Kulkarni G.U.; Thomas J.P. & Edwards P.P. 2000, Metal nanoparticles and their assemblies. *Chem Soc Rev* 29:27–35.

Raveendran P.; Fu J. & Wallen S. L. 2003. Completely "green" synthesis and stabilization of metal nanoparticles. *J Am Chem Soc* 125, 13940-13941

Rodríguez-León E.; Iñiguez-Palomares R.; Navarro R.E. Herrera-Urbina R.; Tánori J.; Iñiguez-Palomares C. & Maldonado A. 2013. Synthesis of silver nanoparticles using reducing agents obtained from natural sources (*Rumex hymenosepalus* extracts). *Nanoscale Res Lett* 8: 318. doi.org/10.1186/1556-276X-8-318.

Rodríguez-Torres M.P.; Acosta-Torres L.S.; Diaz-Torres L. A.; Padron G.H.; Garcia-Contreras R.; Millan-Chiu B. E. 2019. *Artemisia absinthium*-based silver nanoparticles antifungal evaluation against three *Candida* species. *Mater Res Exp* 6(8), 85408. doi:10.1088/2053-1591/ab1fba.

Roux S.; Garcia B.; Bridot J.L.; Salome M.; Marquette C.; Lemelle L.; Gillet P.; Blum L.; Perriat P. & Tillement, O. 2005. Synthesis, characterization of dihydrolipoic acid capped gold nanoparticles, and functionalization by the electroluminescent luminol. *Langmuir* 21, 2526–2536.

Rudge S.; Peterson C.; Vessely C.; Koda J.; Stevens S.; Catterall L. 2001. Adsorption and desorption of chemotherapeutic drugs from a magnetically targeted carrier (MTC). *J Control Release*.74:335–40.

Sabuncu A.C.; Grubbs J.; Qian S.; Abdel-Fattah T.M.; Stacey M.W. & Beskok A. 2012. Probing nanoparticle interactions in cell culture media. *Colloids Surf B Biointerfaces*. 15;95:96-102. doi: 10.1016/j.colsurfb.2012.02.022.

Saif M.J.; Asif H.M.; Naveed M. 2018. Properties and modification methods of halloysite nanotubes: a state-of-the-art review. *Chil Chem Soc* 63: 4109-4125.

Sanvicens N. & Marco M.P. 2008. Multifunctional nanoparticles-properties and prospects for their use in human medicine. *Trends Biotechnol.* 26, 425-433.

- Sathishkumar M.; Sneha K.; Won S.W.; Cho C.W.; Kim S. & Yun Y.S. 2009. Cinnamon zeylanicum bark extract and powder mediated green synthesis of nano-crystalline silver particles and its bactericidal activity. *Colloids Surf B Biointerfaces* 15;73(2):332-8. doi: 10.1016/j.colsurfb.2009.06.005.
- Schultz S.; Smith D.R.; Mock J.J.; Schultz D.A. 2000. Single-target molecule detection with nonbleaching multicolor optical immunolabels. *Proc Natl Acad Sci* 97:996–1001.
- Schulz-Dobrick M.; Sarathy K.V.; Jansen M. 2005. Surfactant-free synthesis and functionalization of gold nanoparticles. *J Am Chem Soc* 127(37):12816-7.
- Sertic, M.; Crkvencic, M.; Mornar, A. Pilepic, K. H.; Nigovic, B.; Males, Z. 2015. Analysis of aucubin and catalpol content in different plant parts of four *Globularia* species. *J Appl Bot Food Qual* 88, 209-214. doi:10.5073/jabfq.2015.088.030.
- Shang L.; Nienhaus K. & Nienhaus G.U. 2014. Engineered nanoparticles interacting with cells: size matters. *J Nanobiotechnol* 3;12:5. doi: 10.1186/1477-3155-12-5.
- Shankar S.S.; Rai A.; Ahmad A. & Sastry M. 2004. Rapid synthesis of Au, Ag, and bimetallic Au core–Ag shell nanoparticles using Neem (*Azadirachta indica*) leaf broth." *J Colloid Interface Sci* 15;275(2):496-502.
- Silva, L.; Rodrigues, A. M.; Ciriani, M.; Fale, P.L.V.; Teixeira, V.; Madeira, P.; Machuqueiro, M.; Pacheco, R.; Florencio, M. H.; Ascensao, L.; et al. 2017. Antiacetylcholinesterase activity and docking studies with chlorogenic acid, cynarin and arzanol from *Helichrysum stoechas* (Lamiaceae). *Med Chem Res* 26(11), 2942-2950. doi:10.1007/s00044-017-1994-7.
- Simpson C.A.; Salleng K.J.; Cliffel D.E.; Feldheim D.L. 2013. *In vivo* toxicity, biodistribution, and clearance of glutathione-coated gold nanoparticles. *Nanomedicine* 9(2):257-63. doi: 10.1016/j.nano.2012.06.002.
- Singh H.; Du J.; Singh P.; Yi T.H. 2018. Role of green silver nanoparticles synthesized from *Symphytum officinale* leaf extract in protection against UVB-induced photoaging. *J Nanostruct Chem* 8: 359. [doi.org/10.1007/s40097-018-0281-6](https://doi.org/10.1007/s40097-018-0281-6).
- Song J.Y. & Kim B.S. 2009. Rapid biological synthesis of silver nanoparticles using plant leaf extracts. *Bioprocess Biosyst Eng* 32.1,79.
- Song S.; Zhao T.; Qiu F.; Zhu W.; Wu Y.; Yanyun J.; Dong L. 2019. Silver nanoparticle decorated halloysite nanotube for efficient antibacterial application. *Chem Phys* 521: 51-54.

Subba R.Y.; Kotakadi V.S.; Prasad, T.V.; Reddy A.V. & Sai Gopal V.R. 2013. Green synthesis and spectral characterization of silver nanoparticles from Lakshmi tulasi (*Ocimum sanctum*) leaf extract. *Spectrochim Acta A: Mol Biomol Spec* 103,156-159. doi:10.1016/j.saa.2012.11.028.

Subrata K.; Sudipa P.; Snigdhamayee P.; Soumen B.; Sujit K.G.; Anjali P. et al. 2007. Anisotropic growth of gold clusters to gold nanocubes under UV irradiation. *Nanotechnology*.18:075712.

Swain P.; Nayak S.K.; Sasmal A.; Behera T.; Barik S.K.; Swain S.K.; Mishra S.S.; Sen AK.; Das J.K. & Jayasankar P. 2014. Antimicrobial activity of metal based nanoparticles against microbes associated with diseases in aquaculture. *World J Microbiol Biotechnol* 30(9):2491-502. doi: 10.1007/s11274-014-1674-4. Epub 2014 Jun 3.

Tahraoui, A.; Israili, Z.H.; Lyoussi, B. 2017. Hypoglycemic and hypolipidemic effects of aqueous extracts of *Ajuga iva* and *Centaurium erythraea* on a rodent model of metabolic syndrome. *Nat Prod J* 7(1), 47-57. doi:10.2174/2210315506666161024122601.

Thipe V.C.; Panjtan A.K.; Bloebaum P.; Raphael K.A.; Khoobchandani M.; Katti K.K.; Jurisson S.S.; Katti K.V. 2019. Development of resveratrol-conjugated gold nanoparticles: interrelationship of increased resveratrol corona on anti-tumor efficacy against breast, pancreatic and prostate cancers. *Int J Nanomedicine* 18; 14:4413-4428. doi: 10.2147/IJN.S204443.

Turkevich J.; Stevenson P.C.; Hillier J. 1951. A study of the nucleation and growth processes in the synthesis of colloidal gold. *Discuss Faraday Soc.*11:55–75.

Velgosova, O. & Veselovsky, L. 2019. Synthesis of Ag nanoparticle using *R. officinalis*, *U. dioica* and *V. vitis-idaea* extracts. *Mater Lett* 248, 150-152. doi:10.1016/j.matlet.2019.04.027.

Von White G.; Kerscher P.; Brown R.M.; Morella J.; McAllister W.; Dean D. & Kitchens C.L. 2012. Green synthesis of robust, biocompatible silver nanoparticles using garlic extract. *J Nanomater.* 2012; 2012. pii: 730746.

Wilton-Ely, J.D.E.T. 2008. The surface functionalisation of gold nanoparticles with metal complexes. *Dalton Trans.* 25–29.

Yu D.G. 2007. Formation of colloidal silver nanoparticles stabilized by Na<sup>+</sup>–poly (γ-glutamic acid)–silver nitrate complex *via* chemical reduction process. *Colloids Surf B: Biointerfaces* 59.2, 171-178.

Zahedifar, M.; Shirani, M.; Akbari, A.; Seyedi, N. 2019. Green synthesis of Ag<sub>2</sub>S nanoparticles on cellulose/Fe<sub>3</sub>O<sub>4</sub> nanocomposite template for catalytic degradation of organic dyes. *Cellulose* 26(11), 6797-6812. doi:10.1007/s10570-019-02550-6.

Zare D.; Khoshnevisan K.; Barkhi M. & Tahami H.V. 2014. Fabrication of capped gold nanoparticles by using various amino acids. *J Experim Nanosci* 9, 957-965. doi.org/10.1080/17458080.2012.752582.

Zeiri Y.; Elia P.; Zach R.; Hazan S.; Kolusheva S. & Porat Z. 2014. Green synthesis of gold nanoparticles using plant extracts as reducing agents. *Int J Nanomedicine* 9, 4007-4021.